

# A Magnetically Torqued Disk Model for Be Stars

J. P. Cassinelli<sup>1</sup>, J. C. Brown<sup>2</sup>, M. Maheswaran<sup>3</sup>, N. A. Miller<sup>1</sup>, and D. C. Telfer<sup>2</sup>

## ABSTRACT

Despite extensive study, the mechanisms by which Be star disks acquire high densities and angular momentum while displaying variability on many time scales are still far from clear. In this paper, we discuss how magnetic torquing may help explain disk formation with the observed quasi-Keplerian (as opposed to expanding) velocity structure and their variability. We focus on the effects of the rapid rotation of Be stars, considering the regime where centrifugal forces provide the dominant radial support of the disk material.

Using a kinematic description of the angular velocity,  $v_\phi(r)$ , in the disk and a parametric model of an aligned field with a strength  $B(r)$  we develop analytic expressions for the disk properties that allow us to estimate the stellar surface field strength necessary to create such a disk for a range of stars on the main-sequence. The fields required to form a disk are compared with the bounds previously derived from photospheric limiting conditions. The model explains why disks are most common for main-sequence stars at about spectral class B2 V. The earlier type stars with very fast and high density winds would require unacceptably strong surface fields ( $> 10^3$  Gauss) to form torqued disks, while the late B stars (with their low mass loss rates) tend to form disks that produce only small fluxes in the dominant Be diagnostics. For stars at B2 V the average surface field required is about 300 Gauss. The predicted disks provide an intrinsic polarization and a flux at H $\alpha$  comparable to observations. The radial extent of our dense quasi-Keplerian disks is compatible with typical estimates. We also discuss whether the effect on field containment of the time dependent accumulation of matter in the flux tubes/disk can help explain some of the observed variability of Be star disks.

*Subject headings:* stars: emission-line, Be – stars: magnetic fields – stars: rotation – stars: winds, outflows – circumstellar matter – polarization

---

<sup>1</sup>Dept. of Astronomy, University of Wisconsin-Madison, 475 N. Charter St. Madison WI 53706; cassinelli@astro.wisc.edu, nmiller@astro.wisc.edu

<sup>2</sup>Dept. of Physics and Astronomy, University of Glasgow, Glasgow G12 8QQ, UK; john@astro.gla.ac.uk, deborah@astro.gla.ac.uk

<sup>3</sup>University of Wisconsin-Marathon County, 518 S. 7th Av. Wausau, WI 54401, mmaheswa@uwc.edu

## 1. Introduction

The presence of disks around rotating stars has long been realized from observations, but has never been explained in a satisfactory way. Particularly pronounced are the disks around the emission line Be stars. These can be detected because of the strong double-peaked emission lines of  $H\alpha$ , large IR continuum excesses, and intrinsic polarizations. Because of these interesting and easily detectable properties, Be stars and their disks have been intensively studied for many years (see reviews in Smith, Henrichs, & Fabregat (2000) and Yudin (2001)). Nevertheless, the origins of their high densities, angular momentum, spatial structure, and variability remain a major puzzle. In addition to the dense equatorial disks, it is well known that Be stars have substantial winds, roughly isotropic, with typical  $\dot{M} \simeq 10^{-(10 \rightarrow 8)} M_{\odot} \text{ yr}^{-1}$  and terminal velocities near  $v_{\infty} \simeq 1000 \text{ km s}^{-1}$  (Marlbrough & Peters 1986; Grady, Bjorkman, & Snow, 1987; Prinja 1989).

Hot stars exhibit rotational line broadening indicative of surface equatorial rotation speeds which are high, but less than about 80 percent the centrifugal (Keplerian) limit. Thus rotation alone is not sufficient to centrifuge material off the equator to form a disk. Owing to the high luminosity of the stars, wind material leaves the general stellar surface due to radiative forces on the line opacity. Line-driving, however, only works well where the wind material is not too optically thick, and has a sufficient velocity gradient for the absorbing atomic lines to sweep through the stellar continuum spectrum. Observational evidence suggests that Be star equatorial disks are too dense and too slowly expanding for line driving alone to support them against gravity.

One possible mechanism proposed to create disks is the Wind Compressed Disk (WCD) model of Bjorkman & Cassinelli (1993). In this, stellar wind matter accelerating out from an intermediate latitude on a rotating star has a trajectory orbital plane which crosses the equatorial plane. The continuous outflows of such matter from the upper and lower hemispheres ‘collide’ in the equatorial plane and form a compressed disk with density enhancement by a factor of  $\sim 100$ , which is on the low side for what is needed observationally. Irrespective of other theoretical issues raised concerning the WCD model (Owocki, Cranmer, & Gayley 1996), the fact is that all the observational indications seem to point toward a disk which is mainly moving azimuthally, supported against gravity by centrifugal forces, i.e., a near Keplerian disk ( $v_r \ll v_{\phi} \approx \sqrt{GM/r}$ ) rather than one which is mainly outflowing ( $v_r \gg v_{\phi}$ ).

The near Keplerian and high density disk inferred from observations poses questions which we address in this paper: How does the material acquire more angular momentum than it possessed when it left the stellar surface? How does such an equatorial disk accumulate material, given that its density and small radial velocity gradient prohibit radiative driving from overcoming gravity in the equatorial plane? Proposed answers to these two

questions have included schemes in which matter is ejected from the star selectively in the pro-grade direction to boost its rotation up to orbital values. In particular, Hanuschik (1999) considered how an outflow of particles with an isotropic Maxwellian distribution could create an orbital regime comprising the faster pro-grade particles with the rest falling back. Owocki & Cranmer (2001) proposed non-radial pulsations with an anisotropic radiation force favoring pro-grade gas flow. While these ideas are interesting, the direct centrifuging action that a strong enough stellar magnetic field could provide seems to be a more direct way of producing the disk.

The possible role of magnetic fields in Be disk production has been mentioned quite often (Friend & MacGregor 1984; Poe & Friend 1986; Ignace, Cassinelli, & Bjorkman 1996). These dealt with applications of magnetic rotator wind theory, which explored the various degrees of control of the outflowing gas by the magnetic fields (Belcher & MacGregor 1976; Hartmann & MacGregor 1982; Poe, Friend & Cassinelli, 1989; Mestel 1990). The magnetic rotator models considered the effects of the field on the azimuthal motion of the gas, the terminal speed of the wind, and the equatorial mass loss rate.

Several papers have discussed aspects of the time-dependent accumulation of stellar wind matter channeled by strong magnetic fields. This has been mainly in the context of early type Chemically Peculiar (CP) stars with very strong magnetic fields (Havnes & Goertz 1984; Babel & Montmerle 1997a), but with ideas being extended recently toward applications to other hot stars and Be star phenomena (Babel & Montmerle 1997b; Donati et al. 2001). Specifically, Havnes and Goertz (1984) discussed the effect of the growing ‘magneto-spheric’ density and mechanisms which might disrupt the field, releasing energy and producing X-rays. Babel and Montmerle (1997a) applied these ideas to develop a magnetically confined wind-shocked model for X-rays from the Ap star IQ Aur and extended this (Babel and Montmerle, 1997b) to the young star  $\theta^1$  Ori C. Donati et al. (2001) applied the model to  $\beta$  Cep which has a magnetic field much lower than those on CP stars, and which, they concluded, is highly oblique to the axis of slow rotation of this star. All of these papers, however, neglected the contribution of rotation to the dynamics of the magnetically channeled wind. This approximation cannot be valid for stars of near critical rotation since the rotational energy density of the channeled wind, and even more so of the shock compressed disk, may far exceed the outflow energy density. Nor can it say anything about how disk material acquires the quasi-Keplerian angular momentum values observed. In this paper we therefore review the problems and address the other limiting regime where the rotational term is dominant (centrifugal force balancing gravity). We do so to evaluate what field is necessary to provide sufficient torquing to produce a dense disk with quasi-Keplerian speeds.

We make use of the fact that near main-sequence B stars have a mass outflow and the

channeling of that flow can lead to shock compressed disk material. The relatively high densities in that disk lead to the strong  $H\alpha$ , excess free-free fluxes and electron scattering polarization for which Be stars are known.

We develop equations to find the field needed both to transfer angular momentum to material that is driven up from the star by line driven wind forces, and to redirect that flow toward the equatorial plane. This regime of a magnetically directed flow is non-spherical and, because there is a build up of matter, is also non-steady. The directed flow results in the formation of a disk-like structure the azimuthal motion of which is ‘quasi-Keplerian’. By this we mean that the velocity distribution is not strictly Keplerian but the motion is primarily azimuthal and with speeds of order the Keplerian value.

We have chosen to use an aligned field of dipole-like shape for the basic magnetic topology,  $\mathbf{B}(r, \theta)$ , with the  $r$ -dependence parameterized. As for the gas, it will for the most part be assumed to be confined by the field. Our main interest is not in the flow trajectories  $\mathbf{v}(r, \theta, \phi)$ , but rather in the azimuthal velocity,  $v_\phi(d)$ , in the equatorial plane at radial distance,  $d$ . The closed field will channel the gas to a specific radial distance,  $d(l)$ , that depends on the latitude  $l$  the field tube had at the stellar surface, the larger  $l$  corresponding to larger  $d$ . Field lines from high latitudes,  $l \gtrsim \pi/4$ , near the pole, would intercept the equator at very large distances, but before reaching those distances the wind energy density will exceed that of the field and no longer be magnetically dominated, since even a dipole field declines as  $d^{-3}$ . Thus, there will be a broad, open, polar wind that fills the envelope volume far beyond the disk and above the closed lines of force that are channeling lower latitude material toward the disk. For our study, we consider both the strictly closed field regions and the transition to the open ones as illustrated in Figure 1.

The simplest picture of the situation would be an abrupt “switch” model, in which the field is assumed to be fully capable of causing solid body rotation,  $v_\phi(d) \propto d$ , out to an Alfvén distance, at which the field energy density has decreased to that in the gas flow. Beyond that transition radius the gas would be dominant and in particular its angular velocity would satisfy conservation of angular momentum,  $v_\phi \propto 1/d$ . In this representation, there is a discontinuous shift in  $v_\phi(d)$  (from  $v_\phi \propto d$  to  $v_\phi \propto d^{-1}$ ). Although this picture may be useful for understanding some basic concepts involved in the torquing of disks, we know from magnetic rotator stellar wind theory that no such abrupt shift occurs at the Alfvén point in either  $v_\phi$  or the angular momentum.

To allow for a more realistic behavior of the angular speed and angular momentum transfer, we introduce a “smooth transition” model, in which a continuous parametric function,  $v_\phi(d)$  is specified for the angular velocity as a function of distance in the equatorial plane. This function reaches a maximum, but the angular momentum continues to increase

with increasing radius by a factor of about two, transmitted by the bent field lines. We are interested in cases in which  $v_\phi(d)$  reaches at least to the Keplerian speed  $v_K = \sqrt{GM/d}$ . The field lines will not be considered drawn open until at least a distance,  $d_{\text{outer}}$ , where the Keplerian ratio, i.e.  $v_\phi(d)/v_K(d)$  is at its maximal value. The maximal Keplerian ratio radius is identified with the Alfvén radius and, from that radius outward, we assume that the gas motion then tends to the field-free flow limit. Thus, at large  $d$ , it obeys conservation of angular momentum, and the particles remain in their orbital planes defined at the point where they became free from the magnetic field forces.

The subsequent flow trajectories in the far field region become similar to those in wind compression theory, either in the form of the WCD model or the Wind Compressed Zone (WCZ) model of Ignace, Cassinelli, & Bjorkman (1996). The WCZ model was developed to describe the structure of a wind which has a rotation that is too slow to form a shock compressed disk, but nonetheless can produce density enhancements in the low latitude regions. The enhancements in density (by a factor of 10 or so) have an effect on the observational properties of a wide range of stars. The field lines are drawn out in the far field regime as described by Ignace, Cassinelli, & Bjorkman (1998). Neither the WCD nor the WCZ models can explain the quasi-Keplerian disks of Be stars.

The relation to WCD theory of the current model for a shock compressed disk is as follows. The WCD model is “kinematic” in that the *radial velocity structure* of the outflow is chosen to obey the well-known beta law distribution, instead of being computed from the force of radiation on line opacities. In WCD theory, the velocity component  $v_\phi$  is assumed to be determined by conservation of angular momentum, and thus  $v_\phi$  decreases rapidly with radius and does not attain the quasi-Keplerian angular speeds inferred from observations. In the current paper, we again use a kinematic approach, but now specify an *azimuthal velocity structure*,  $v_\phi(d)$ , that assures quasi-Keplerian velocities are reached for a sufficiently strong magnetic field. This kinematic approach allows us to derive constraints on the surface field,  $B_\circ$ , and the surface spin rate parameter,  $\mathcal{S}_\circ$ , that are needed for a disk to form. Mass and magnetic flux conservation requirements provide information regarding the disk density distribution, the radial extent, and the timescale for variability. Where needed we also use the wind beta velocity law to provide an estimate of the flow velocities driven by the star’s radiation field. The derived structure for stars with “torqued disks” allows us to estimate observational properties such as H $\alpha$  line strengths, intrinsic polarizations, and continuum fluxes at a variety of wavelengths useful for comparisons of the model with observations.

A major goal is to derive lower limits on the field strengths required for the existence of centrifugally-supported disks produced by an aligned dipole-like field on a Be star. As a first rough estimate, showing that the fields required to channel a flow are not unreasonable,

we consider magnetic rotator wind theory. In that theory, as explained in Ch 9 in Lamers & Cassinelli (1999) (hereafter L&C), there is a “primary mass loss mechanism” (in our case the line driven wind theory), which sets the stellar mass loss rate, and the terminal velocity. An amplification of both  $\dot{M}$  and  $v_\infty$  can be produced by the co-rotating magnetic field. A transition occurs from the case in which the field acceleration effect is unimportant (a “slow magnetic rotator”) to the case in which the field produces a strong effect (a “fast magnetic rotator”, or FMR). This transition occurs when the Michel velocity,  $V_M$ , (which is very close to the terminal velocity in FMR theory) is as large as the terminal velocity owing to the primary mass loss mechanism. The Michel velocity is related to the Poynting flux which makes the enhanced outflow energetically possible. As a starting point, we consider it reasonable to assume that the field necessary to dominate the flow and channel it to the equatorial disk should be at least comparable to the transition field strength from slow to fast magnetic rotator theory for a particular star. The Michel Velocity,  $V_M$ , is given by quantities defined at the surface of the star; the surface field, ( $B_\circ$ ), rotation rate ( $\Omega_\circ$ ), and mass loss rate,  $\dot{M}$ . Solving for  $B_\circ$  in the equation for  $V_M$  gives a minimal field based on FMR considerations.

$$B_{\text{FMR}} = \frac{(\dot{M}V_M^3)^{1/2}}{R^2\Omega_\circ} \quad (1)$$

$$\approx \frac{(\dot{M}v_\infty^3)^{1/2}}{\mathcal{S}_\circ\sqrt{RGM}} \quad (2)$$

$$= 6.9 \text{ Gauss} \frac{\dot{M}_{-9}^{1/2} v_8^{3/2}}{\mathcal{S}_\circ(R_{12}M_{10})^{1/2}} \quad (3)$$

where  $R$  is the stellar radius. We set  $R\Omega_\circ$  equal to the surface equatorial speed  $v_\circ$ , which is expressed as the equatorial Keplerian speed,  $v_K(R)$  times a fraction  $\mathcal{S}_\circ$ . We also set  $V_M = v_\infty \approx v_E$  (where  $v_E$  is the escape speed at the stellar surface). For numerical values, we express the velocity by the ratio  $v_8 = v_\infty/(10^8 \text{ cm s}^{-1})$ ; the stellar mass and radius ratios by  $M_{10} = M/(10M_\odot)$ ,  $R_{12} = R/(10^{12} \text{ cm})$ ; and the mass loss rate by  $\dot{M}_{-9} = \dot{M}/(10^{-9} M_\odot \text{ yr}^{-1})$ .

A roughly similar value for the magnetic field, as in Equation (3), follows from requiring that the energy density of the surface field  $B_\circ^2/8\pi$  should exceed that of the gas  $\rho_\circ v_\circ^2/2$ . The derived field of order 10 Gauss (for  $\mathcal{S}_\circ \simeq 1$ ) is a very modest one. However, as we shall see, it is a lower bound on  $B_\circ$  because it effectively uses the density in the wind, which is much below (i.e.  $\simeq 10^{-3}$ – $10^{-4} \times$ ) the densities that are produced in the centrifugally supported disk, so that the field ( $\propto \rho^{1/2}$ ) torquing the disk is 30 to 100 times larger than that in Equation (3).

## 2. Schematic Description of the Model

Let us start by considering the case of a non-rotating star with a strong surface magnetic field, which we take to be of dipole-like form (but of more a general  $r$ -dependence), and with a uniform wind mass flux,  $\mathcal{F}_{M,o} = \dot{M}/(4\pi R^2)$ , from its surface. If we consider starting from a vacuum environment and initiate an outflow, gas will be channeled along the field lines (assuming  $\frac{1}{2}\rho v_w^2 \ll B^2/8\pi$ ), and along with matter from the opposite hemisphere, tend to fill the flux tubes to ever greater distances with wind compressed gas, creating an extended dense disk. This is the non-rotating case considered by Babel & Montmerle (1997a). The flux tubes would fill toward pressure balance. However, the resulting decrease in the velocity gradient would probably quench radiative driving, tending to cause the matter to fall back, although Babel & Montmerle (1997a) suggest otherwise. We suspect that the Rayleigh Taylor instability might be important and prevent a wind flow from supporting a relatively dense envelope against gravity.

When we introduce rotation, the magnetic field exerts an azimuthal force on the gas as well as acting to constrain its radial flow path to be along the flow tubes. As is illustrated in Figure 1, the latitude  $l$  at which the flow originates will determine the azimuthal velocity of matter as it is channeled into the equatorial disk. Matter originating in some latitude range  $l_1 < l < l_2$  will tend to reach the equator at  $d_{\text{inner}} < d < d_{\text{outer}}$  with moderate speeds  $v_{\parallel}$  parallel to the field lines in the corotating frame. As a result of the influx of matter, there will be a build up of mass in these sectors of the disk. Although compressed to high densities by the shock fronts of the incident flows, the material in the disk will be supported against infall mostly by centrifugal forces.

We discuss below the parameters of the various resulting regions in the equatorial plane, and also the timescale on which they change. We find the latter to be long compared to typical rotation periods. So, for the purposes of this paper, we assume we have reached a nearly steady stage of moderately dense disk creation and consider the effect of stellar rotation.

Most of our interest is in the collision of winds in the equatorial plane, which involves material that is near and above the local Keplerian speed. Therefore, we find it convenient to express equations in terms of the dimensionless equatorial distance variable  $x = d/R$ , and the variable  $\mathcal{S}(x) = v_{\phi}(x)/v_K(x)$ , which is the ratio of the azimuthal speed to the local Keplerian speed  $v_K(x)$ . A fundamental parameter for a specific star is the “stellar spin rate parameter”  $\mathcal{S}_o$ , which is the ratio  $v_o/v_K(R)$  of the stellar rotation speed to the Keplerian velocity at the stellar equator; thus  $\mathcal{S}_o = \mathcal{S}(\text{at } x = 1)$ . In principle,  $\mathcal{S}_o$  can have values in the range  $0 \leq \mathcal{S}_o \leq 1$ . However, for most Be stars the range is  $0.6 \lesssim \mathcal{S}_o \lesssim 0.8$ . We assume for simplicity that the star is spherical and not distorted by the rotation.

### 3. Existence and Extent of Magnetically Centrifuged Disk

We begin by finding a form for  $v_\phi(d)$  that is consistent with known magnetically centrifuged wind systems and provides a kinematic distribution that we can use at all distances. Although the topology of the field in the rotating dipole case is very different, there are properties of the azimuthal velocity that should carry over from magnetic rotator theory (L&C Chapter 9). At small radii, the azimuthal speed behaves as in the solid body case, i.e.  $v_\phi \propto d$ , while farther out it satisfies the conservation of angular momentum relation  $v_\phi \propto 1/d$ . Now let us find a kinematic expression for  $v_\phi$ , that is valid both near and far from the star and also provides a continuous form that asymptotically matches both behaviors.

#### 3.1. The Description of the Angular Velocity, $v_\phi(x)$ , in the Disk

At small distances from the star where the field is strong, we expect the azimuthal speed of disk matter to be controlled by centrifuging, i.e., to follow the co-rotation distribution

$$v_\phi \simeq v_o x \quad (x \gtrsim 1) \quad (4)$$

Farther out, the angular velocity in the region well beyond the Alfvén distance should follow the conservation of angular momentum expression  $v_\phi = (v_{\phi,\text{peak}} d_{\text{peak}})/d$ , where  $v_{\phi,\text{peak}}$  is the maximum  $v_\phi(d)$ , which occurs at  $d = d_{\text{peak}}$ . We express  $d_{\text{peak}}$  in terms of the dimensionless parameter,  $\alpha$ , where

$$\alpha = d_{\text{peak}}/R = x_{\text{peak}} \quad (5)$$

and thus  $v_{\phi,\text{peak}} \approx v_o \alpha$ . At large  $x$  we will have

$$v_\phi(x) \simeq \frac{v_o \alpha^2}{x} \quad (x > 1, x \gg x_{\text{peak}}) \quad (6)$$

At intermediate equatorial distances, the exact form of  $v_\phi(x)$  depends on details of how the field bends in reaction to the inertia of the matter. However, a reasonable form for  $v_\phi(x)$  parameterized by  $\alpha$ , and which has the limiting behaviors (4) and (6), is

$$\frac{v_\phi(x)}{v_o} = \frac{\alpha^2 + 1}{\frac{\alpha^2}{x} + x} \quad (7)$$

where the numerator normalizes  $v_\phi(x)$  so that  $v_\phi(x = 1) = v_o$ . This analytic form proves convenient for exploring the properties of the disk driving regime. Although Equation (7) is



purely empirical, it is designed to reflect the actual behavior of matter torqued in a magnetic field.

Figure 2 shows  $v_\phi(x)$  from Equation (7) for various  $\alpha$  values, as functions of  $x$ . Speeds are shown relative to  $v_\circ$ , so the relative height of  $v_\phi(x)$  and  $v_K(x)$  depend on  $\mathcal{S}_\circ$ .

While it is interesting to see the dependence of the adopted  $v_\phi(x)$  distribution on  $\alpha$ , we will see later that  $\alpha$  is not a fundamental stellar parameter comparable to the rotation quantity  $\mathcal{S}_\circ$ . In fact, for a star with a given  $\dot{M}$  and  $v_\infty$ , the location  $x = \alpha$  of the peak of the curve itself depends on  $\mathcal{S}_\circ$  as well as on the field  $B_\circ$  at the surface of the star. Only after we explore the consequences of assuming Equation (7) for  $v_\phi(x)$ , and particular forms for the disk field and density distributions, will we be able to identify the various independent stellar parameters for the Be star disk problem.

Two other curves of interest are also shown in Figure 2: the Keplerian circular velocity,  $v_K(x)$  and the escape speed  $v_E(x)$ , where

$$v_K(x) = \frac{1}{\sqrt{2}}v_E(x) = \sqrt{\frac{GM}{Rx}} = \frac{v_\circ}{\mathcal{S}_\circ x^{1/2}} \quad (8)$$

We need to compare the angular speed,  $v_\phi$  with the local Keplerian speed, so it is convenient to use the Keplerian ratio ( $\mathcal{S}(x) = v_\phi(x)/v_K(x)$ ) introduced previously. Using Equation (7) we get

$$\frac{\mathcal{S}(x)}{\mathcal{S}_\circ} = \frac{v_\phi(x)x^{1/2}}{v_\circ} = \frac{(\alpha^2 + 1)x^{3/2}}{\alpha^2 + x^2} \quad (9)$$

This reaches a maximum at  $x = \sqrt{3}\alpha$ . Figure 3 shows  $\mathcal{S}(x)$  versus  $x$ , for various  $\alpha$  values. Of particular interest is the value of  $\alpha$  for which  $\mathcal{S}$  just tangentially reaches unity, i.e. for which there is just a single point at which the angular speed reaches the Keplerian speed. This “Threshold value” of  $\alpha$  is called “ $\alpha_{\text{Th}}$ ”, and it occurs at  $x_{\text{Th}} = \sqrt{3}\alpha_{\text{Th}}$ . For a given star,  $\alpha_{\text{Th}}$  will determine the minimal magnetic field that is required to produce a torqued disk, i.e. one with material having angular velocities at least as large as Keplerian speed.

Figures 2 and 3 reveal a number of regimes of behavior according to the value of  $\alpha$ ,

1. For the ‘weak’ field regime, curves of type *I*, with ( $\alpha < \alpha_{\text{Th}}$ ) never produce a  $v_\phi(x)$  value as high as  $v_K$  at any  $x$ , so  $\mathcal{S} < 1$  at all  $x$ . The centrifugal force supplied by magnetic torquing to material originating at any latitude is not able to overcome gravity. We assume that the matter will tend to fall back to the star unless supported by other forces such as radiation pressure or ram pressure of the inflowing accumulating gas.

Field lines will already be bent by the inertia of the gas at radial distances close to the stellar surface.

2. For a “moderate” field regime, for which  $\alpha_{\text{Th}} \leq \alpha \lesssim 3$  (depending on  $\mathcal{S}_o$ ) is of most interest in producing quasi-Keplerian disks. The surface fields at intermediate  $l$  are strong enough to centrifuge gas to equal (critical curve *A*) or exceed (curves of type *II*) the Keplerian circular speed  $v_K(x)$ . This range in  $\alpha$  will result in a quasi-Keplerian disk over a range  $x_{\text{inner}}$  to  $x_{\text{outer}}$ . The distance  $x_{\text{inner}}$  is the first point at which the material has a speed greater than the Keplerian speed, and we choose  $x_{\text{outer}}$  to be the distance at which the Keplerian ratio  $\mathcal{S}$  is maximal and at which we can consider the field to lose its dominance over the gas flow.
3. For the “large” magnetic field regime (curves of type *III* for which  $\alpha \gg \alpha_{\text{Th}}$ ), the magnetic torquing gives the matter sufficient  $v_\phi$  alone to equal escape speed. However, the field could still dominate and prevent outflow. Beyond some large distance, outflow is assumed to occur with little further increase in angular momentum and the angular velocity will vary as  $x^{-1}$ . Arbitrarily large  $\alpha$  could centrifuge and contain a disk of arbitrary radial extent. However,  $\alpha$  depends on the surface field for which there are bounds as described by Maheswaran & Cassinelli (1988, 1992), so there are in fact upper bounds to  $\alpha$  as well.

We should also emphasize that even though the curves of  $v_\phi$  in Figure 2 have the appearance of trajectories, they are *not* matter trajectories, but rather give the azimuthal velocities of matter which has arrived at a particular distance  $x$  in the equatorial plane, having originated from latitude  $l$ .

### 3.2. Boundaries and Regions of the Disk

Here we derive expressions for the limiting radii of particular interest to the torqued disk problem. The innermost distance of interest,  $x_{\text{inner}}$ , is that at which the torqued matter first attains the local Keplerian speed. It occurs where  $\mathcal{S} = 1$ . So by Equation (9),  $x_{\text{inner}}$  is the solution of

$$\frac{(\alpha^2 + 1)x_{\text{inner}}^{3/2}}{\alpha^2 + x_{\text{inner}}^2} = \frac{1}{\mathcal{S}_o} \quad (10)$$

This non-linear equation can be solved by a Newton iteration, which converges quickly when we start with the large  $\alpha$  solution to Equation (10), i.e.  $x_{\text{inner}} \simeq \mathcal{S}_o^{-2/3}$ . Figure 4 shows

$x_{\text{inner}}(\alpha, \mathcal{S}_o)$  versus  $\alpha$  for various  $\mathcal{S}_o$ , (0.5, 0.7, 0.9).

The next distance of interest is where  $v_\phi$  peaks, namely  $d_{\text{peak}} = x_{\text{peak}} R$ , which we have already seen is given by

$$x_{\text{peak}} = \alpha \quad (11)$$

and at which the rotation speed ratio is

$$\frac{v_\phi(x_{\text{peak}})}{v_o} = \frac{\alpha^2 + 1}{2\alpha}. \quad (12)$$

To define an outer radius of the torqued disk we need a criterion to decide where the quasi-Keplerian disk torquing effectively ceases. For this we adopt the distance at which the ratio  $\mathcal{S}(x)$  maximizes, i.e. where  $d\mathcal{S}/dx = 0$ , for a fixed  $\alpha$ . From differentiation of Equation (9) this is found to be

$$x_{\text{outer}} = \sqrt{3}\alpha \quad (13)$$

The value of  $v_\phi$  at  $x_{\text{outer}}$  is given by

$$\frac{v_\phi(x_{\text{outer}})}{v_o} = \sqrt{3} \frac{\alpha^2 + 1}{4\alpha} \quad (14)$$

which for large  $\alpha$  varies as  $\sim 0.43\alpha$ . Thus, both the location and velocity at the peak increase roughly linearly with the parameter  $\alpha$ . Note that although  $x_{\text{outer}}$  is not explicitly dependent on  $\mathcal{S}_o$ , it depends on  $\mathcal{S}_o$  through  $\alpha(\mathcal{S}_o)$ .

A key issue is the minimum value of  $\alpha$  for which a Keplerian regime exists at all. There is a single point at which the angular speed just reaches the Keplerian speed. Setting  $\mathcal{S} = 1$  at  $x = \sqrt{3}\alpha$  in Equation (9) gives

$$\alpha_{\text{Th}}^{3/2} + \frac{1}{\alpha_{\text{Th}}^{1/2}} = \frac{4}{3^{3/4}\mathcal{S}_o} \quad (15)$$

This minimal or “threshold” value of  $\alpha$ , produces a Keplerian value of  $v_\phi$  at the singular distance  $x_{\text{Th}} = \sqrt{3}\alpha_{\text{Th}}$ . In Figure 5 we show the numerical solution for  $\alpha_{\text{Th}}(\mathcal{S}_o)$  obtained from Equation (15). This equation shows that  $\alpha_{\text{Th}}$  will be less than 1 for values of  $\mathcal{S}_o$  larger than  $2/(3^{3/4}) \approx 0.9$  (also shown in Figure 5). However, it should be noted that at very large spin rates the star will be substantially non-spherical and our whole treatment becomes rather approximate. Our results should be regarded as most reliable for values of  $\mathcal{S}_o$  that are less than 0.9.

We observe from Figure 5 that for the  $\mathcal{S}_o$  range most relevant to Be stars, an excellent fit to the solution is

$$\alpha_{\text{Tth}} \approx \mathcal{S}_o^{-K}; \quad \text{where } K \simeq 0.88 \quad (16)$$

shown as the dashed line in Figure 5.

To relate  $\alpha$  to absolute scales of  $B$ ,  $\rho$ , and  $\mathcal{S}_o$ , we will adopt  $x = x_{\text{outer}} = \sqrt{3}\alpha$  as the point where  $B^2/8\pi \simeq \rho v_\phi^2/2$ , i.e. we take  $x_{\text{outer}}$  to be the Alfvén distance. Therefore, our definition of the Alfvén distance leads to the relation

$$x_{\text{Alf}} = x_{\text{outer}} = \sqrt{3}\alpha \quad \text{for } \alpha \geq \alpha_{\text{Tth}} \quad (17)$$

Thus, the Alfvén distance is the outer boundary of our torqued disk.

We recognize that there is a degree of arbitrariness with this definition of the Alfvén distance. However, just as we were guided by wind theory in our choice of the kinematic expression for the angular velocity, we can also get some insight from magnetic rotator winds regarding an appropriate definition of the Alfvén radius. In the case of winds the Alfvén radius does not correspond to the peak of the  $v_\phi(x)$  distribution, but as seen in L&C, Fig 9.3, occurs farther out because the field continues to contribute to the speed of the gas. The peak of our  $\mathcal{S}$  curve (at  $x = \sqrt{3}\alpha$ ) clearly lies farther out than the maximum in the  $v_\phi$  curve (at  $x = \alpha$ ). It corresponds to an extremum in the torquing of the disks, in that no further increase in the Keplerian ratio occurs. However, perhaps the best reasons for choosing the maximum in  $\mathcal{S}$  to be the outer boundary of a disk are seen by considering the threshold case in which the  $\mathcal{S}$  curve just tangentially reaches unity, which occurs for  $\alpha = \alpha_{\text{Tth}}$  and at the location,  $x_{\text{Tth}}$ . By definition of “a threshold distance” we would want the inner and outer boundaries to coincide, and the condition  $x_{\text{inner}} = x_{\text{outer}}$  occurs at  $x_{\text{Tth}}$ . The tangentially Keplerian point is also an important location because the components of the total velocity ( $v_r, v_\theta, v_\phi$ ) are fully definable for the first time at  $x_{\text{Tth}}$ : The radial velocity,  $v_r$  equals zero at the equatorial extremity of the dipolar field. The polar velocity  $v_\theta$  is there nulled by the collision between the oppositely directed streams. The tangential velocity there is  $v_\phi = v_K(x_{\text{Tth}})$ , so  $v_{\text{total}}(x_{\text{Tth}}) = v_\phi(x_{\text{Tth}})$ . Furthermore, using shock conditions we will find the distance  $x_{\text{Tth}}$  to be the first radial distance in the equator for which our marginal model leads to a quasi-Keplerian disk density ( $\rho_D$ ). Therefore, all the quantities needed for giving an equality between the total speed and an Alfvén speed,  $B/\sqrt{4\pi\rho}$ , are definable at  $x_{\text{Tth}}$ . Thus we will be able to use the conditions at  $x_{\text{Tth}}$  to define a threshold surface field  $B_{o,\text{Tth}}$  required to produce a torqued disk.

Choosing the peak of  $\mathcal{S}$  to define the outer boundary of the torqued disk and also the

Alfvén radius will allow us to predict the dependence of observational fluxes on field strengths and intrinsic stellar properties. We will then be able to test the resulting models against general Be and hot-star observational requirements.

We assume that, beyond  $x_{\text{outer}} (= x_{\text{Alf}})$ , the gas flow will tend to draw the field outward and change from being predominantly an azimuthal flow to dominantly an outflow in the form of field-free WCD or WCZ trajectories. The flow will make the transition to a nearly radial wind as the latitude of the point of origin increases. For  $\alpha > \alpha_{\text{Th}}$ , the ‘Keplerian disk’ regime extends from  $d = x_{\text{inner}} R$  (Equation 10) to  $d = x_{\text{outer}} R$  (Equation 13). Beyond the distance  $x_{\text{outer}} = \sqrt{3}\alpha$ , the flow is no longer controlled by the field and there is a transition from a quasi Keplerian to an outflow dominated velocity structure.

To get numerical values for these various boundaries in  $x$ , we need to specify how the magnitude of  $B(x)$ , and  $\rho(x)$  vary with distance, for a given value of  $\mathcal{S}_\circ$ . Since  $\alpha$  depends on  $\mathcal{S}_\circ$ , as well as on  $B$  and  $\rho$ , we specify all of these quantities in Section 4. To get a rough idea at present of the expected disk extent, we take  $\mathcal{S}_\circ=0.7$  and assume that  $B$  and  $\rho$  are such that  $\alpha = 2$ . Applying Equations (10) and (13), we find the range of the quasi-Keplerian disk to be  $1.45R \lesssim d \lesssim 3.46R$ ; a plausible range for Be star disks.

## 4. The Distribution of $B(x)$ and $\rho(x)$ in the Equatorial Disk

### 4.1. Distribution of $B(d)$

We choose to represent the field in the system as having a topology similar to the dipole limit, but to allow for greater generality we use a parameterized rate of decline with distance  $d$ . Specifically we set

$$B(d) = B_\circ \left( \frac{d}{R} \right)^{-b} = B_\circ x^{-b} \quad (1 \leq x \leq x_{\text{outer}}) \quad (18)$$

where  $B_\circ = B(R)$  is the value at the stellar surface. In fact, the disk does not extend down to  $x = 1$  but only to  $x = x_{\text{inner}}$ . Beyond  $x = x_{\text{outer}}$  the field lines tend to stretch and break open and we do not attempt to describe this here as it is not inside the torqued disk regime. As we will show, the field within the disk determines its radial extent. We also need to know the shape of the field lines in the region out of the equatorial plane. This is because it is the frozen-in *tube geometry* between the footprint of the field at stellar latitude  $l$ , and the point  $x(l)$  where the field crosses the disk which determines the *flow geometry* (i.e. area of the tubes) through which the wind mass flux is channeled.

To get the tube geometry, we make the simplifying approximation that the field strength (and also the wind mass flux) is uniform over the surface of the star, i.e.  $B_{\circ}$  is assumed to be the field at all  $l$ , and the field lines are normal to the stellar surface. These assumptions — as well as constant radial  $\mathbf{B}$  and constant mass flux - will not be strictly true in a rapidly rotating star, but they should be adequate to describe the limited range of latitudes  $l$  that adds matter to the range  $x_{\text{inner}}$  to  $x_{\text{outer}}$  in the disk.

With these assumptions regarding the field geometry, the outgoing cross-section of a flux tube of area  $A_{\circ}$  at the stellar surface has a value  $A$  at  $d$  in the equatorial plane determined by field line conservation to be

$$A(d) = A_{\circ} \frac{B_{\circ}}{B(d)} = A_{\circ} x^b \quad (19)$$

where we have used Equation (18) for the ratio of the fields at the base and at the point of intersection with the disk.

## 4.2. The Density Structure, $\rho_D(d)$ , of the Disk

We assume that the density is determined by pressure balance in the post shock region where the flows from the upper and lower hemispheres collide. Thus, the density near the equatorial plane is determined in much the same way as in Bjorkman & Cassinelli (1993), but the material is not flowing outward, in contrast with the WCD model. Also, since the material has an angular velocity at or above the Keplerian speed, it is supported against gravity by centrifugal forces. Thus the dynamic pressure does not also need to support the gas against gravity, which is the case for the models of the slowly rotating chemically peculiar stars (Babel & Montmerle 1997a).

The opposing wind streams provide a ram pressure that must be balanced by the static gas pressure in the shock compressed region. The density in the shock compressed disk can be significantly larger than that in the incident winds, especially in the near-equator zone where the shocked gas has cooled radiatively. We can assume the equatorial disk region to be cool ( $\approx 10^4$  K) because such a temperature can be maintained from a radiative equilibrium balance with the incident stellar radiation field. That is, the density is sufficiently high that radiative cooling is effective and sufficient to balance the heating by the stellar light. For a Be star, the appropriate temperature range is from 1 to  $2 \times 10^4$  K, and with the corresponding sound speed  $c_s = (kT/\mu m_H)^{1/2}$ , where  $\mu m_H$  is the mean particle mass. We find by equating the disk gas pressure to the wind ram pressure that,

$$\rho_D(x)c_S^2 = \rho_w(x)v_w^2(x) = \mathcal{F}_M(x)v_w(x) \quad (20)$$

where  $\rho_w$  and  $v_w$  are the density and velocity of the flow at the equatorial end of the magnetic tube, and  $\mathcal{F}_M(x)$  is the mass flux there. We use the subscript,  $w$  (for wind), on both the incident velocity and density. We assume that the radiation forces drive a field-channeled flow with a parallel velocity,  $v_{\parallel}$  which is comparable to the wind speed that could have been reached at a radial distance  $d$  in the line driven wind of a non-magnetic B-star. We take this to be given by the beta law expression

$$v_w(d) = v_{\infty} \left(1 - \frac{R}{d}\right)^{\beta} \quad (21)$$

The mass loss rate of the B-star sets the surface mass flux scale  $\mathcal{F}_M$ , and as stated above it is sufficient for our purposes to assume the mass flux rate  $\mathcal{F}_{M,o} = \mathcal{F}_M(x=1)$  is the same at all latitudes on the star. The mass flux at  $x$  is related to the mass flux entering at the star via  $\mathcal{F}_M(x) \times A(x) = \mathcal{F}_{M,o} \times A_o$ , where  $A$  is the area perpendicular to the flux tubes, as given in (19). Thus we obtain,

$$\mathcal{F}_M(x) = \frac{\dot{M}}{4\pi R^2} x^{-b} \quad (22)$$

$$= 5.02 \times 10^{-9} (\text{gm cm}^{-2} \text{ s}^{-1}) \frac{\dot{M}_{-9}}{R_{12}^2} x^{-b} \quad (23)$$

Using Equations (21) and (22), the disk density at the equator is given by the pressure balance equation (20), thus

$$\rho_D(x) = \frac{\dot{M}v_w(x)}{4\pi R^2 c_S^2} x^{-b} \quad (24)$$

$$= \frac{\dot{M}}{4\pi R^2 v_{\infty}} \left(\frac{v_{\infty}}{c_S}\right)^2 (1 - 1/x)^{\beta} x^{-b} \quad (25)$$

$$= \rho_c \left(\frac{v_{\infty}}{c_S}\right)^2 (1 - 1/x)^{\beta} x^{-b} \quad (26)$$

$$= 3.04 \times 10^{-13} \text{ gm cm}^{-3} \frac{\dot{M}_{-9} v_8}{R_{12}^2 T_4} (1 - 1/x)^{\beta} x^{-b} \quad (27)$$

where we let

$$\rho_c \equiv \dot{M}/(4\pi R^2 v_{\infty}) = 5.02 \times 10^{-17} \text{ gm cm}^{-3} \frac{\dot{M}_{-9}}{R_{12}^2 v_8} \quad (28)$$

be a characteristic stellar mass loss density, and

$$\rho_{D,c} \equiv \rho_c (v_\infty/c_S)^2 = 6.06 \times 10^3 \rho_c \left( \frac{v_8^2}{T_4} \right) \quad (29)$$

be the characteristic density in the disk. The corresponding number densities are given by  $n_c = \rho_c/(\mu m_H)$  and  $n_{D,c} = \rho_{D,c}/(\mu m_H)$ .

From differentiation of Equation (24), we find that the disk density peaks at  $x = 1 + \beta/b \leq 1 + \beta/3$  which lies close to  $x_{\text{inner}}$ , i.e.

$$\rho_{D\text{MAX}} = \rho_{D,c} \frac{b^b \beta^\beta}{(b + \beta)^{b+\beta}} = 3.04 \times 10^{-13} \frac{b^b \beta^\beta}{(b + \beta)^{b+\beta}} \frac{\dot{M}_{-9} v_8}{R_{12}^2 T_4} \quad (30)$$

The disk density in Equation (27) is nearly 4 orders of magnitude larger than that in the “wind” incident on the disk

$$\rho_w(x) = \frac{\mathcal{F}_M(x)}{v_w} \simeq \frac{\dot{M}}{4\pi R^2 v_w(x)} x^{-b} = \rho_c \frac{v_\infty}{v_w(x)} x^{-b} \quad (31)$$

$$= 5.02 \times 10^{-17} \text{gm cm}^{-3} \frac{\dot{M}_{-9}}{R_{12}^2 v_8} (1 - 1/x)^{-\beta} x^{-b} \quad (32)$$

Thus the two adjacent densities (post- and pre-shock) given by Equations (27) and (31) respectively, differ by about a characteristic Mach number squared  $(v_\infty/c_S)^2$ , as is typically the case for isothermal shocks. In the case of early-type stars such as the Be stars, the Mach number factor is quite large. Finally, the large density contrast between the region in and out of the shocked disk justifies the neglect of gas pressure compared with the centrifugal support, as assumed in our model.

## 5. The Magnetic Field for Disk Production in Terms of Stellar Parameters

### 5.1. The Alfvén Distance and the Minimal Field to Produce a Disk

We now have explicit parameterizations of the disk field,  $B(x)$  (Equation 18), density  $\rho_D(x)$  (Equation 24), and azimuthal velocity (Equation 7) as functions of  $x$ . Given these, we can explicitly find the minimum or threshold surface field,  $B_{o,\text{Th}}$ , needed to torque a quasi-Keplerian disk, and the extent of the disk, as functions of the stellar spin rate,  $\mathcal{S}_o$ , and wind properties,  $\dot{M}$ ,  $\beta$ , and  $v_\infty$ . The existence of unique solutions for  $B_{o,\text{Th}}$  and for disk



inner and outer radii depends on the facts that  $v_\phi(x)$  increases with  $x$  in the inner region and so can exceed  $v_K$  if  $B$  is strong enough, and that  $B^2(x)/4\pi\rho_D$  declines monotonically with  $x$ , so that the torquing effect of the field turns off at some sufficiently large  $x$ . It is easy to confirm that Equations (18), (24), and (7) satisfy this monotonic decline in energy density ratio.

To express  $\alpha$  explicitly in terms of the physical parameters of the star, we use the fact that at the rotational Alfvén point,  $x_{\text{Alf}} (= x_{\text{outer}})$ ,

$$\frac{B^2(x_{\text{Alf}})}{8\pi} = \frac{1}{2}\rho_D(x_{\text{Alf}})v_\phi^2(x_{\text{Alf}}) \quad (33)$$

which, on using Equations (18, 24, and 7) implies that

$$x_{\text{Alf}}^{b+2} \left(1 - \frac{1}{x_{\text{Alf}}}\right)^\beta \frac{(\alpha^2 + 1)^2}{(\alpha^2 + x_{\text{Alf}}^2)^2} = \frac{B_o^2}{4\pi\rho_c} \frac{R}{GM} \left(\frac{c_S}{v_\infty}\right)^2 \frac{1}{\mathcal{S}_o^2} \quad (34)$$

Using  $x_{\text{Alf}} = \sqrt{3}\alpha$  (Equation (17)), and substituting this in Equation (34) gives us

$$\frac{3^{\frac{b}{2}+1}}{16} \alpha^{b-2} (\alpha^2 + 1)^2 \left(1 - \frac{1}{\sqrt{3}\alpha}\right)^\beta = \Gamma^2 \quad (35)$$

where we use the definition

$$\Gamma^2 \equiv \frac{B_o^2}{4\pi\rho_c} \frac{R}{GM} \frac{c_S^2}{v_\infty^2} \frac{1}{\mathcal{S}_o^2} \quad (36)$$

$$= \frac{\gamma^2}{\mathcal{S}_o^2} \frac{c_S^2}{v_\infty^2} \quad (37)$$

Equation (35) is our basic equation for relating  $\alpha$ , the fundamental quantity in our kinematic model, to the stellar field and basic stellar properties contained in  $\Gamma$ . In Figure 6, we show  $\Gamma(\alpha)$  from Equation (35) for several  $b$  values (3, 6, 9) with  $\beta = 1$ , while illustrating a range of  $\beta$  values (0.5, 1.0, 2.0) for the pure dipole-field case ( $b = 3$ ). Note that

$$\gamma = \left[ \frac{\frac{B_o^2}{8\pi}}{\frac{GM\rho_c}{2R}} \right]^{\frac{1}{2}}. \quad (38)$$

Therefore,  $\gamma$  is a measure of the magnetic energy density to gravitational energy density of the wind material near the stellar surface, and depends only on  $B_o$ ,  $M/R \times \dot{M}/v_\infty$ . Thus  $\gamma$

is essentially the ratio of the surface Alfvén speed at the density of the wind to the surface Keplerian speed. On the other hand,  $\mathcal{S}_o$  is simply the ratio of surface rotation speed to surface Kepler speed, so the right-hand side of Equation (35) (i.e.  $\Gamma$ ) involves only velocity ratios at the star while the left-hand side contains only the model parameter  $\alpha$  plus the wind  $\beta$  value, which is known (*i.e.*  $\simeq 1.0$ ), and  $b$  which parameterizes the rate of decline of the field and we know  $b \geq 3$ . Note in particular that we can identify,  $\gamma$ ,  $v_\infty/c_S$  and  $\mathcal{S}_o$  as independent and fundamental parameters, whereas the kinematic description parameter  $\alpha$  is not fundamental, as  $\alpha = \alpha(\gamma, v_\infty/c_S, \mathcal{S}_o)$ .

## 5.2. The Fundamental Stellar Parameters for Disk Production

We can now translate the analysis of the disk, in §3, in terms of kinematic parameter  $\alpha$  into the real physical parameters of different stars.

First of all, we can find the surface field  $B_{o, \text{Th}}$  needed to create a quasi-Keplerian disk for a star of given  $\mathcal{S}_o$ ,  $M$ ,  $R$ ,  $\dot{M}$ ,  $v_\infty$ , and  $\beta$ . To do so we use the results of Figure 5 (from Equations 15 and 16) to obtain  $\alpha_{\text{Th}}(\mathcal{S}_o)$  for the given  $\mathcal{S}_o$  value. We can then use  $\alpha_{\text{Th}}$  in Equation (35) (with the chosen values of the parameters  $b$ , and  $\beta$ ) to obtain  $\Gamma_{\text{Th}}(\mathcal{S}_o)$  which is a convenient intermediate variable encompassing all of the velocity ratios of the system.

Given  $\Gamma_{\text{Th}}$  from  $\alpha_{\text{Th}}$  for the chosen  $\beta$  and  $b$  and using Equation (28) for  $\rho_c$ , we can now find

$$B_{o, \text{Th}} = \mathcal{S}_o \Gamma_{\text{Th}}(\mathcal{S}_o) \left( \frac{GM\dot{M}v_\infty}{R^3 c_S^2} \right)^{\frac{1}{2}} \quad (39)$$

$$= \mathcal{S}_o \Gamma_{\text{Th}}(\mathcal{S}_o) \times Y_* \quad (40)$$

where  $Y_*$  is determined by stellar properties.

Using the reference values for  $M$ ,  $R$ ,  $\dot{M}$ , and  $v_\infty$  introduced for Equation (3) while introducing  $c_S = 1.3 \times 10^6 T_4^{1/2}$ , Equation (39) can be expressed numerically as

$$Y_* = 71 \text{ Gauss} \left( \frac{M_{10} \dot{M}_{-9} v_8}{R_{12}^3 T_4} \right)^{\frac{1}{2}} \quad (41)$$

In principle we should solve Equation (15) to get  $\alpha_{\text{Th}}(\mathcal{S}_o)$  and hence  $\Gamma_{\text{Th}}(\mathcal{S}_o)$ , but we noted that Equation (16) ( $\alpha = \mathcal{S}_o^{-K}$ ) yields an excellent empirical fit to  $\alpha_{\text{Th}}(\mathcal{S}_o)$ . Using the

empirical fit in Equation (36) gives

$$\Gamma_{\text{Th}}(\mathcal{S}_o) = \frac{3^{b/4+1/2}}{4} \mathcal{S}_o^{-K(b/2-1)} (\mathcal{S}_o^{-2K} + 1) \left(1 - \frac{\mathcal{S}_o^K}{\sqrt{3}}\right)^{\beta/2} \quad (42)$$

which we show in Figure 7 along with the exact solution of Equation (15).

Inserting  $K = 0.88$  explicitly in Equations (39) and (42) for the range of  $\mathcal{S}_o$  of greatest interest for Be stars we get,

$$B_{o,\text{Th}}(\mathcal{S}_o) = 17.5 \text{ Gauss} \times 3^{b/4+1/2} \mathcal{S}_o^{1.88-0.44b} (\mathcal{S}_o^{-1.76} + 1) \left(1 - \frac{\mathcal{S}_o^{0.88}}{\sqrt{3}}\right)^{\beta/2} \left(\frac{M_{10}\dot{M}_{-9}v_8}{R_{12}^3 T_4}\right)^{\frac{1}{2}} \quad (43)$$

Figure 8 shows  $B_{o,\text{Th}}$  versus  $\mathcal{S}_o$  for a B2 V star for various values of  $b$  and  $\beta$ . For the dipole case ( $b = 3$ ) the threshold surface field for a star rotating at  $\mathcal{S}_o=0.7$  is about 250 Gauss. If the field drops off more rapidly with distance from the star, a significantly larger surface field is required to produce the disk. Primarily this is because the inner boundary, which is identical to  $x_{\text{Alf}}$  for  $B_{o,\text{Th}}$ , is not at the stellar surface but at 2.43 R, so for the larger values of  $b$ , a larger surface field is needed to give the same field at  $x_{\text{Alf}}$ . The effect of changing the wind velocity law index is shown by the curves labeled with various values of  $\beta$  in Figure 8, and these indicate that the steepness of the wind velocity law is also of some importance in determining the field strengths required to produce a disk. For example, in the case with  $\mathcal{S}_o=0.7$ , a slowly-accelerating flow with  $\beta = 2$  can be channeled to the equator by a field only 70% as strong as that needed for the more-quickly-accelerating  $\beta = 0.5$  case.

## 6. Properties of a Torqued Quasi-Keplerian Disk

### 6.1. Hot Main-Sequence Stars and the Possibilities for Disk Production

To see how  $B_{o,\text{Th}}$  depends on stellar parameters we note that  $M$ ,  $R$ ,  $\dot{M}$ ,  $v_\infty$ , along the main sequence are all essentially determined by the spectral type  $T_{\text{eff}}$  as given in a table from Bjorkman & Cassinelli (1993). Table 1 gives the factor  $Y_*$  in Equation (35) which isolates the field dependence on stellar properties. Adopting  $b = 3$  and  $\beta = 1$  we can then find  $B_{o,\text{Th}}(\mathcal{S}_o)$  as a function of  $T_{\text{eff}}$  from Equation (35). Table 1 also includes representative values of  $B_{o,\text{Th}}$  for  $\mathcal{S}_o=0.5, 0.7, 0.9$ .

Figure 9 shows the comparison the minimal field from Equation (43) along with the

bounds on stellar magnetic fields that were derived by Maheswaran & Cassinelli (1988, 1992). The latter bounds were derived from considerations of envelope circulation currents and maximal contributions of field pressure to hydrostatic support. We can see in Figure 9 that very large magnetic fields are required to produce disks around O stars. Such large fields are needed because the large wind momenta ( $\dot{M}v_\infty$ ) of O-star require large magnetic forces to deflect their flows. For the case of the O3 V star the required field lies above the maximal allowed field for many different stellar spin rates. For the early B stars with a spin rate of  $\mathcal{S}_o = 0.7$  the field required is in the range 100 to 1000 Gauss. Such fields are small enough to have avoided detection in the past, but are near the field strength recently found by Donati et al. (2001) in  $\beta$  Cep. For the late B stars, we see that because of their small wind momentum rates, rather weak dipole fields of order 30 Gauss could produce a torqued disk. In such cases we need to know if the predicted disks would be detectable.

The properties of the stars in Table 1 lead to specific predictions regarding the disk extent and observational diagnostics should vary with stellar parameters. In particular, for given values of  $b, \beta, M, R$ , we expect the radial extent of the quasi-Keplerian disk to increase with increased  $B_o$  while decreasing with increased  $\dot{M}v_\infty$ , predictions that might be observationally testable. We now investigate the radial extent of disks as function of stellar magnetic field, and find the number of particles in the disk to find if the model can explain the polarimetric properties and disk emission measures, which determine the H $\alpha$  fluxes, of Be stars.

## 6.2. Radial Extent

In Section 3 we obtained expressions in terms of  $\alpha, \mathcal{S}_o$ , for the radial extent of the disk,  $x_{\text{inner}} \rightarrow x_{\text{outer}}$ . This extent is of course zero for  $B_o \leq B_{o,\text{Th}}$ . For  $B_o > B_{o,\text{Th}}$ , we can obtain explicit values for  $x_{\text{inner}}$  and  $x_{\text{outer}}$ , in terms of  $B_o, \mathcal{S}_o$  and other stellar parameters ( $M, R, \dot{M}, v_\infty, T$ ), by translation from  $\alpha$  to  $\Gamma$  using (38). Specifically, for any given set of stellar parameters  $Y_*$ , we can calculate  $\Gamma$  and then obtain the corresponding  $\alpha$  (for given  $\beta, b$ ) from Figure 6, or by numerical inversion of (38). Then we have  $x_{\text{outer}} = x_{\text{Alf}} = \sqrt{3}\alpha$ . Here we illustrate results by adopting  $b = 3, \beta = 1$ , and deriving  $x_{\text{inner}}$  and  $x_{\text{outer}}$  as functions of  $\mathcal{S}_o$  and the ratio  $B_o/Y_*$ .

The results are shown in Figure 10. Figure 10a shows that results for three values of  $\mathcal{S}_o$ . On this panel, it is easy to see that  $\mathcal{S}_o$  sets the threshold for the field needed to produce a disk. This figure also shows that for values of  $B/Y_*$  slightly above the threshold field, the disk extent increases sharply, and in a seemingly homologous way vs.  $\mathcal{S}_o$ . To check the apparent homology we show in Figure 10b the ratio of  $x_{\text{inner}}$  and  $x_{\text{outer}}$  expressed in terms of

threshold radii  $x_{\text{Th}}$  versus the ratio of  $B/B_{\text{o,Th}}$ .

As for the inner boundary, the position  $x_{\text{inner}}$  denotes the position in the disk where the material first reaches the Keplerian speed (i.e.  $\mathcal{S} = 1$ ). For the minimum surface field which will accelerate material to Keplerian speed ( $B_{\text{o,Th}}$ ), the disk material reaches Keplerian speed at only one point,  $x_{\text{inner}} = x_{\text{outer}} = \sqrt{3}\alpha$ . The other point on the kinematic  $v_\phi$  curve in Figure 2 where the speed is Keplerian is of no interest because it is beyond the torqued disk outer boundary, where the field is no longer dominant in determining the disk's  $v_\phi(x)$  structure.

Note in Figure 10 that, for values of  $B_{\text{o}}$  large enough to enforce nearly solid body rotation, the location of the inner boundary is nearly independent of the magnetic field, as it is primarily set by the value of  $\mathcal{S}_{\text{o}}$  as mentioned earlier. In regards to the outer boundary, an expression for  $B_{\text{o}}/B_{\text{o,Th}}$  can be derived from the ratio of two values of  $\Gamma^2$  in Equation (36), evaluated at  $\alpha = x_{\text{Alf}}/\sqrt{3}$  and at  $\alpha = x_{\text{Th}}/\sqrt{3}$ , and we find that the outer radius varies with  $B_{\text{o}}/B_{\text{o,Th}}$ , roughly as  $x_{\text{Alf}}/x_{\text{Th}} \sim (B_{\text{o}}/B_{\text{o,Th}})^{2/5}$ . The net effect is that the outer boundary and the extent of the disk increases as  $B_{\text{o}}$  increases, but the location of the inner boundary does not change much.

From an observational point of view these considerations only concern the magnetically torqued regions while the flow in the far regions could also show enhanced densities because of the WCD effects as schematically illustrated in Figure 1.

The typical range of the disk model boundaries here is of the same order with  $x_{\text{outer}} \sim 3$  to 10, as discussed in the empirical models of Be stars assuming Keplerian disks and based on IRAS observations (Waters 1986), and H $\alpha$  line observations by Côté, Waters, & Marlborough (1996). As the latter authors note, the observations do not rule out disks of greater radial extent, since the tenuous outer parts contribute little to the polarization or emission measure. Indeed some observations such as the radio observations of Taylor et al. (1990) show that high density material can reach distances of order 100  $R$ . The bulk of this extent might be a tenuous outflow WCD/WCZ region as opposed to a quasi-Keplerian one.

Now we have the physical boundaries of a Magnetically Torqued Disk and expressions for the density distribution in the disk so it is possible to test if the predicted disk satisfies basic observational limits, especially in regards to the classic Be star diagnostics provided by polarization and H $\alpha$  observations.

## 7. Comparisons with Observations

### 7.1. Continuum Scattering Polarization

One important diagnostic of the Be disk properties is the polarization they produce by electron scattering. Using the Brown & McLean (1977) general theory of (single) scattering polarization, one finds that for a disk of approximately uniform thickness  $H$  and a density distribution given by Equation (34) for  $x_{\text{inner}} \leq x \leq x_{\text{outer}}$ , the resulting polarization is

$$p = \frac{3}{32} \frac{\sigma_T}{\pi} \int_{x_{\text{inner}}}^{x_{\text{outer}}} n_e(x) \mathcal{D}(x) H dx / x \quad (44)$$

Here  $\sigma_T$  is the Thomson cross section,  $n_e$  is the electron number density ( $= \rho_D / \mu m_H$ ), and we ignore absorption and assume the disk is fully ionized. Here we have included the finite source depolarization factor,  $\mathcal{D}$  of Cassinelli, Nordsieck, & Murison (1987), and Brown, Carlaw, & Cassinelli (1991), and assumed an edge-on aspect angle. Equation (44) yields, for  $n_e(x)$  given by Equation (24)

$$p = \frac{3\sigma_T H}{32\pi} n_{D,c} I_p \quad (45)$$

where the integral

$$I_p = \int_{1/x_{\text{outer}}}^{1/x_{\text{inner}}} y^{b-1} (1-y)^{\beta+1/2} dy \quad (46)$$

can be expressed in terms of incomplete Beta functions.

For  $x_{\text{outer}} \gg 1$ ,  $\beta = 0.5$ , and  $b = 3$ , the integral  $I_p \approx 1/(2x_{\text{inner}}^2) - 1/(3x_{\text{outer}}^3) \approx 0.1$  for typical  $x_{\text{inner}}$ . Using Equation (24) for the disk density in Equation (45), the resulting numerical value for the polarization is given by:

$$p(\%) \simeq 0.5 \left( \frac{n_{D,c}}{10^{11}} \right) R_{12} \times \frac{H}{R} \quad (47)$$

Using the theoretical disk number density from Equation (24)

$$n(x) = n_{D,c} x^{-b} (1 - 1/x)^\beta = 1.8 \times 10^{11} \text{cm}^{-3} \frac{\dot{M}_{-9} v_8 x^{-b} (1 - 1/x)^\beta}{R_{12}^2 T_4}, \quad (48)$$

then Equation (47) produces  $p \simeq 1\%$  for the scale values  $\dot{M}_{-9}, R_{12}, v_8, T_4$  all = 1. Polarizations of about 1% are typical for the intrinsic polarizations of Be stars (McLean & Brown 1978).

## 7.2. Disk Emission Measure and Luminosity

Key signatures of the presence of dense disks include the emission in Balmer lines and the IR continuum excess over that from the stellar photosphere. The relation between these emission properties, the disk density structure, and the continuum polarization has been discussed by various authors (e.g. Waters & Marlborough 1992; Bjorkman & Cassinelli 1990, Yudin 2001, Wood, Bjorkman, & Bjorkman 1997). Here, as another check of our derived density distribution, we estimate the line and continuum emission that is expected. Both the Balmer lines and the IR continuum emission arise collisionally, so at moderate optical depths their luminosities  $L$  take the form  $L = 4\pi j \times EM$ , where  $EM = \int_V n^2 dV$  is the emission measure of source volume  $V$ , and  $j$  is the appropriate emission coefficient in [ergs cm<sup>3</sup> s<sup>-1</sup>] for each process, which we assume to be constant through the source volume  $V$  since the cooled post-shock disk is taken to be isothermal. We assume the disk has a roughly constant thickness  $H$  at all distances from  $x_{\text{inner}}$  to  $x_{\text{outer}}$ , and use the density distribution in Equation (30) for  $\rho_D(x)$ , to find

$$EM = 2\pi R^2 H \int_{x_{\text{inner}}}^{x_{\text{outer}}} n_D^2 dx \quad (49)$$

$$= 2\pi R^2 H I_L n_{D,c}^2 \quad (50)$$

$$= I_L \times EM_o \quad (51)$$

where  $I_L$  is given by

$$I_L(b, \beta, x_{\text{inner}}, x_{\text{outer}}) = \int_{x_{\text{inner}}}^{x_{\text{outer}}} x^{-2b+1} \left(1 - \frac{1}{x}\right)^{2\beta} dx \quad (52)$$

The integral  $I_L$  can be expressed in terms of incomplete beta functions. For integer  $b$  and half integer  $\beta$  it can be evaluated analytically and we find it insensitive to  $\beta$  and to  $x_{\text{Alf}} \gg 1$ . For  $b = 3$  its value is in the range  $I_L = (1 - 5) \times 10^{-2}$  for  $2 > x_{\text{inner}} > 1$ . The scale emission measure  $EM_o$  is

$$EM_o = 2\pi R^2 H n_{D,c}^2 \quad (53)$$

$$= \frac{1}{8\pi} \frac{H}{R} \left[ \frac{\dot{M} v_\infty}{R^{1/2} c_S^2 m_H} \right]^2 \quad (54)$$

$$= 2.3 \times 10^{61} \text{ cm}^{-3} \frac{H}{R} \left[ \frac{\dot{M}_{-9} v_8}{T_4 R_{12}^{1/2}} \right]^2 \quad (55)$$

If we use an approximate value for the emissivity,  $4\pi j_{\text{H}\alpha} = 2.4 \times 10^{-25} \text{ergs cm}^3 \text{s}^{-1}$  (Osterbrock 1989) we find the line luminosity,  $L(\text{H}\alpha) = 4\pi j_{\text{H}\alpha} \times EM$  to be

$$L(\text{H}\alpha) = 6.3 \times 10^{36} \text{erg s}^{-1} \frac{H}{R} \left[ \frac{\dot{M}_{-9}^2 v_8^2}{R_{12} T_4^2} \right] I_L \quad (56)$$

Also of interest is the comparison of the line luminosity  $L(\text{H}\alpha)$  with the stellar continuum  $L_\lambda$  at the  $\text{H}\alpha$  line wavelength. For the purposes here the stellar continuum luminosity can be approximated by the Rayleigh-Jeans distribution  $B_\lambda^{RJ}(T)$ . Thus the monochromatic stellar continuum luminosity at  $\text{H}\alpha$  is

$$L_\lambda^* \approx \frac{8\pi^2 R^2 c k T}{\lambda^4} \quad (57)$$

This yields the optically thin line equivalent width  $W_\lambda = L(\text{H}\alpha)/L_\lambda^*(T)$  using Equations (57) and (56) to be

$$W_\lambda = \frac{I_L}{64\pi^3} \frac{4\pi j_{\text{H}\alpha} \lambda^4}{c} \frac{H}{R} \frac{\dot{M}^2 v_\infty^2}{R^3 (kT)^3} \quad (58)$$

giving, for  $I_L \approx 0.05$

$$W_\lambda = 1.3 \text{ \AA} \frac{H}{R} \left( \frac{\dot{M}_{-9}^2 v_8^2}{R_{12}^3 T_4^3} \right) \quad (59)$$

For larger  $\dot{M}$  stars this yields a huge value for  $W_\lambda$  since we have ignored attenuation. We roughly correct for this by evaluating

$$W'_\lambda = W_\lambda e^{-\tau} \quad (60)$$

and use an approximate disk electron scattering optical depth

$$\tau \approx n_o R \sigma_T \approx 0.1 \frac{\dot{M}_{-9} v_8}{R_{12} T_4} \quad (61)$$

Results for  $\tau$ ,  $W'_\lambda$  versus spectral type  $T_{\text{eff}}$  are given in Table 2 and shown in Figure 12. For stars with higher  $T_{\text{eff}}$  the high disk optical depth can suppress  $W'_\lambda$  while for the lower  $T_{\text{eff}}$  the low density results in small  $W_\lambda$  even before optical depth effects are taken into account. According to this model, only a narrow range of  $T_{\text{eff}}$  around that of early B stars should



show an easily detectable  $H\alpha$  line. Observationally, Jaschek & Jaschek (1983) found that the frequency of Be stars as a function of spectral type peaks at spectral class B2, and a similar result is seen in the IRAS survey of B stars by Coté & Waters (1997). Equivalent widths of  $H\alpha$  range from a few Å to about 30 Å (Coté et al. 1996; Coté & Waters 1997). The Magnetically Torqued Disk model predicts roughly the right emission line properties, although clearly a better treatment of the radiation transfer is required. Also the Be phenomenon extends to late B stars, so a reason for the wide range of spectral classes that contain Be stars needs to be explored in the context of our model. We now consider the implications of this model for the qualitatively different phenomenon, the variability of the Be stars on a variety of time scales.

### 7.3. Time Variable Phenomena

Undoubtedly many of the chief clues to the dynamical structure of Be star disks come from the complex time variability of these objects. Be stars vary on a wide range of characteristic times from “activity” on scales of hours (Balona 2000) to quasi-periodic variability on years to decades (Doazan 1982). Also of interest is the phase transition time from non-emission line to emission line phases that indicate disks can vanish and re-appear on time intervals of hundreds of days, (Hubert-Delplace et al. 1982 and Hubert 1981; Dachs 1987). The connection between our Magnetically Torqued Disk (MTD) model and these time scales is discussed below in § 7.3.1. In addition to changes in overall line strength, another interesting source of variability in these objects is the cyclic change in the strengths of the violet and red peaks of the  $H\alpha$  emission lines, known as V/R variation. This phenomenon comprises a shifting asymmetry of emission line peaks from  $V$  to  $R$  over a timescale of order a decade (Telting et al. 1994; Telting 2000). Ideas for understanding the  $V/R$  variations within the context of the MTD model are discussed in § 7.3.2

#### 7.3.1. Time Development of Disk Thickness

Our interest has been in finding the field strength required to have matter transmitted from the star to the relatively dense disk inferred from observations. Later we mention some ideas for modifying our basic model to produce a gas dominated disk that seems to be required for the one armed instability to operate.

As can be seen in Equation (59), we can attribute time variability of  $H\alpha$ , to the time dependent increase in the height of the disk,  $H(t)$ , so we need an expression relating the

time derivative  $dH/dt$  to stellar parameters. We first note that the mass inside a disk area element  $A(d)$  at any time is  $\rho(d)A(d)H$ . Both  $\rho(d)$  and  $A(d)$  should not change appreciably in our rigid field model. If we equate the change in this mass to the mass influx from the magnetically channeled wind, we obtain

$$\rho A(d) \frac{dH}{dt} = \mathcal{F}_M(d) A(d) \quad (62)$$

where  $\rho(d) = \mathcal{F}_M(d)v_w(d)/c_S^2$  and we get

$$\frac{dH}{dt} = \frac{c_S^2}{v_w} = 0.52 \times 10^{12} \text{ cm/year} \frac{T_4}{v_8} \quad (63)$$

Let us consider the time for the star to change from the non emission phase to an emission phase Be star. For this let us assume the lines are noticeable when the equivalent width is about 1 Å. Therefore, setting  $W_\lambda = 1.0$  in Equation (59), we obtain from  $H(t) = (dH/dt) \times t_1$ , the start-up time,

$$t_1 = 1.5 \text{ years} \frac{R_{12}^4 T_4^2}{\dot{M}_{-9} v_8} \quad (64)$$

For the values associated with a B2 star, and with  $T_4 = 0.8T_{\text{eff}}$  this gives a reasonable value of about 4 months. For later type B stars, the value increases significantly (100 years in the case of a B5V stars and  $10^3$  years at B9V). These long times for the late B stars is mostly because the mass loss rates we assumed for these stars are much lower, and hence  $t_1$  in Equation (64) is longer. Although there is a known a tendency for later B stars to change on a slower time scale (Hubert-Delpace et al. 1981), we suggest that a better agreement of our model with the observations of the late B stars would occur if we accounted for the extreme version of FMR theory that was called “Centrifugal Magnetic Rotator” theory (L & C, §9.7.1 and Figure 9.7). In this class of magnetic rotator winds the mass loss rate is enhanced because the density scale height in the subsonic and solid body portion of the wind is increased by centrifugal forces and  $\dot{M}$  increases exponentially with  $\mathcal{S}_o^2$  (L & C, Eq 9.90). The late Be stars appear to have a larger  $\mathcal{S}_o$  on average than do the early Be stars (Hubert-Delpace et al. 1981), and would be the ones for which centrifugal magnetic rotator effects are likely to be important. If late Be stars have mass loss rates in excess of those predicted by pure line driving, our estimate for the disk start-up timescale could be brought to an reasonable range.

In our model, the height of the disk would increase linearly with time, so a growth-time scale can be defined as  $t_G = 1/(d \ln H/dt)$ . Of particular interest in this regard is the fill-up

time  $t_{fill}$ . This is the time it takes the incident mass flux to increase the height  $H$  of disk matter in the tube to its maximal value which is about  $d$  (c.f. Donati et al. 2001 discussion). Thus

$$t_{fill} \simeq \frac{d}{\frac{dH}{dt}} = \frac{d}{v_w} \left( \frac{v_w}{c_S} \right)^2 = t_{Flow} \left( \frac{v_w}{c_S} \right)^2 x \quad (65)$$

$$\simeq 2.1 \text{ years} \frac{R_{12} v_8}{T_4} \times x \quad (66)$$

Made without considering detailed mechanisms, this estimate of the disk filling time is much longer than the wind flow time ( $t_{Flow} = R/v_\infty$ ). The disk filling time is about four years in the inner disk ( $x \simeq 2$ ), with the outer regions eventually filling in around a decade—tantalizingly close to the observed long term Be star disk variability time scales. Some discussion of specific field disruption mechanisms (reconnection, diffusion) by matter accumulation is to be found in Havnes & Goertz (1984), Babel & Montmerle (1997a), and Donati et al. (2001).

### 7.3.2. Connections with the $V/R$ Variations

The interpretation of the  $V/R$  variations proposed by Papaloizou et al. (1992) and Okazaki (1991) is that the variation is due to the very slow rotation/precession of an azimuthally localized density enhancement in the disk across the line of sight from the approaching to the receding part of the disk. The physical model proposed for such a density enhancement and drift is that it is a density wave in the disk, somewhat like galactic spiral density waves, but attributable to the gravitational field of the non-spherical central star, rather than to self-gravitation (negligible in a stellar disk). This model is attractive in predicting a density spiral precession period of the right order for typical Keplerian speeds. The MTD model discussed here shares some important features with the models of precessing one-armed spirals. Most importantly, both models envision a disk in which material spends a long time in roughly Keplerian motion (in fact, the observations of  $V/R$  variations are often cited as evidence of the existence of a near-Keplerian disk).

The  $V/R$  variability on irregular time scales of average 7 years (Okazaki 1997) has been explained as the orbital motion of a one armed spiral pattern in a disk. A model by Lee, Saio, & Osaki (1991) has proposed that the matter is driven up from the star by viscosity. A one armed pattern in the disk has been explained by the Global Disk Oscillation model of Okazaki (1991, 1996) and Papaloizou et al. (1992). The GDO model would operate in quasi-Keplerian disks but not in disks in which the material has a short residence time. Matter

must be supplied to the disk either continually or by events such as non-radial pulsations that occur on a time scale shorter than the viscous time scale as considered by Owocki & Cranmer (2001).

The V/R phenomenon is one that all models must try to address. In our magnetic channeling/torquing model, for strong fields a substantial part of the disk would have corotating  $v_\phi$  values and one might expect the field torquing forces to overwhelm any gravitational density wave effect, though in the outer disk where the field will bend (attaining a  $\phi$  component) there might be some such effect. Any concentration of disk density by a stellar surface field that is not uniform in  $\phi$  would be expected roughly to corotate with the star, rather than over long periods. This is therefore an intriguing open question for future consideration.

A very interesting idea, proposed by H. Henrichs (2002, private communication), is that the stellar field might be time variable. During periods when it is strong our model would apply and a dense disk would build up over the fill time we estimated. However as it stands the model provides no obvious way to explain  $V/R$  variations, at least via density wave precession in a Keplerian disk controlled by the gravity of the non-spherical star. If, however, the field weakened substantially then the disk would decouple from the field and become near Keplerian through viscous effects and capable of supporting such density waves until the field returned or the disk decayed - another observed phenomenon the timescale of which requires explanation. This idea makes the testable prediction that  $V/R$  variations should be absent during disk build up and present only at times of weak field.

## 8. Discussion

The central point of our model is that magnetic torquing and channeling of wind flow from the intermediate latitudes on a B star can, for plausible field strengths, create a dense disk a few stellar radii in extent in which the velocity is azimuthal and of order the local Keplerian speed. The model was motivated by the fact that line profile data (e.g. Hanuschik 1996) indicate that disk emission lines of Fe II, extend to  $\Delta v > v_o \sin i$ , and reach disk Keplerian values. Also the sharp absorption features seen in the center of those lines do not show evidence for inflow or outflow. The latter of course would be expected in the case of the WCD model. The present paper aimed to show that fields could confine and torque the flow to create a quasi-Keplerian disk of roughly the spatial extent suggested by these observations. Future work to test the real viability of the model will address two important questions:

- a) Is the azimuthal velocity distribution  $v_\phi(d)$  across the radial range of the dense disk

predicted by our magnetic model compatible with observed line profiles? This model distribution starts as roughly corotational, i.e.  $v_\phi(d) \propto d$ , and transitions to a  $v_\phi$  decreasing with  $d$ . This distribution is clearly not truly Keplerian disk  $v_\phi(d) \propto 1/\sqrt{d}$ . However, the typical  $v_\phi$  is comparable with  $v_K$  and exists over only a rather narrow range of  $d$ , unless the field is very strong, which is unlikely on theoretical grounds (Maheswaran & Cassinelli 1988, 1992; c.f. Figure 9). Outside the model disk domain, i.e. at  $x > x_{\text{AIF}}$ , we predict quantitatively a somewhat flattened WCD region changing with increasing  $d$  to a WCZ. At even farther distances from the star, the wind will be nearly spherical. All of these regions involve strong outflow velocities but with densities much below those in the quasi-Keplerian disk. It is important to estimate whether the high  $v_r$  but low density distributions there are compatible with line profile data i.e. does there exist an outer expanding flattened disk which affects line profiles very little but is detectable by radio observations etc. These and other diagnostic predictions of the Magnetically Torqued Disk model such as X-ray production will be treated in subsequent papers.

- d) Another issue, that is perhaps related to the  $V/R$  variations is the winding up of the field - something we have ignored so far. In a model with strictly corotational  $v_\phi(r) = v_\phi R/R$  out to some point and angular momentum conservation beyond there, the field would corotate in the disk region. However, in practice and for our parametric model (Equation 7),  $v_\phi(r)$  falls behind corotation and the field will be wound up. The resulting  $B_\phi$  component will have opposite sign on opposite sides of the disk plane and will grow until field reconnection can occur allowing a quasi-steady state with the disk matter slipping across the field lines. In such a situation gravitational control of the disk may dominate sufficiently for the disk to behave as quasi-Keplerian and allow density waves. Indeed, in the light of this, one might argue that our estimate of  $B_{\phi, \text{Th}}$  is too conservative since the crucial feature of our model is that the field should deliver wind matter to the disk with sufficient angular momentum (from magnetic torquing) and with essentially no  $v_r$  but only  $v_\theta$  so that shock compression can occur without any outflow (in contrast to the WCD model). This needs working out in detail but if only the wind density needs torquing action our field limits would be much reduced. Furthermore, in that case the disk  $\rho_D v_\phi^2$  would be so high compared to  $B^2/8\pi$  that the matter would completely dominate the field once delivered into the dense disk, which would consequently be essentially Keplerian and so support density waves under the action of stellar gravity.

In this paper we have followed a used a kinematic description of the azimuthal velocity of a disk zone, along with constraints based on magnetic rotator theory to develop an

analytic model which we call the Magnetically Torqued Disk (MTD) model. We derived the independent parameters for disk formation problem: the spin rate parameter,  $\mathcal{S}_o$ , the surface field  $B_{o,Th}$  and the stellar parameters contained in the quantity,  $Y_*$ . We assumed a rather simple rigid magnetic field picture, but one that allowed us to derive an estimate of the field required to produce a torqued disk for main sequence stars ranging from O3 V to B9 V. Although an unreasonably large field was found to be needed for the early O stars, we concluded that at the early B spectral class at which the Be phenomena are most prominent, the model provided about the right observational properties, and for reasonable surface field strength. Also, we considered several time scales associated with Be stars, and found start-up, growth and fill-up time scales that are in the month to decade long range that seem appropriate. For the late B stars the start-up time scale and the  $H\alpha$  equivalent widths appear to be small and we suggest that perhaps the mass loss rates for these stars need to be enhanced by centrifugal magnetic rotator forces. Modifications that are needed to address V/R variations and observational consequences at a variety of wavelengths will be considered in later papers.

We gratefully acknowledge the financial support of a PPARC Fellowship (JPC) and PPARC Grant (JCB), Studentship (DCT) and NSF grant AST-0098597 (JPC). The paper has benefited from discussions with J. Mathis, R. Hanuschik, L. Oskina, J. Bjorkman, and A. Lazarian.

## REFERENCES

- Babel, J. & Montmerle, T. 1997a, *A&A*, 323, 121
- Babel, J. & Montmerle, T. 1997b, *ApJ*, 485, L29
- Balona, L. A., . 2000, in *IAU Coll. 175, ASP Conf Ser. 214, The Be Phenomenon in Early Type Stars*, eds. M. A. Smith & H. F. Henrichs (ASP), 1
- Belcher, J. W., MacGregor, K. B. 1976 *ApJ*, 210, 498
- Bjorkman, J. E., & Cassinelli, J. P. 1993, *ApJ*, 409, 429
- Bjorkman, J. E., & Cassinelli, J. P. 1990, in *Angular Momentum and Mass Loss for Hot Stars*, ed. L. A. Wilson & R. Stalio (Ames, IA: Reidel Pub. Co.), 185
- Brown, J. C., & Carlaw, V. A., & Cassinelli, J.P. 1989 *ApJ*, 344,341
- Brown, J. C., & McLean, I. S. 1977, *A&A*, 57, 141
- Cassinelli, J. P., Nordsieck, K., & Murison, M. A. 1987, *ApJ*, 317, 290

- Coté, J., Waters, L. B. F. M. & Marlborough J. M. 1996, *A&A*, 307, 184
- Coté, J., & Waters, L. B. F. M. 1997 *A&A*, 176, 93
- Dachs, J. 1987 in *IAU Colloq. 92, Physics of Be Stars* (Cambridge: Cambridge Univ. Press), 149
- Doazan, V. (1982) in *B stars with and without Emission Lines, Monograph Series on Non-thermal Phenomena in Stellar Atmospheres*, eds, A. Underhill and V Doazan, NASA SP-456 (CNRS-NASA) p 277
- Donati, J.-F., Wade, G. A., Babel, J., Henrichs, H. F., de Jong, J. A., Harries, T. J. 2001, *MNRAS*, 326, 1265
- Friend, D. B. & MacGregor, K. B. 1984, *ApJ*, 282, 591
- Grady, C. A., Bjorkman, K. S., & Snow, T. P. 1987, in *IAU Colloq. 92, Physics of Be Stars* (Cambridge: Cambridge Univ. Press), 268
- Hanuschik, R. W. 1999, private communication
- Hartmann, L., & MacGregor, K. B. 1982 *ApJ*, 259, 180
- Havnes, O., & Goertz, C. K. 1984, *A&A*, 138, 421
- Hubert-Delplace, Hubert, H. 1981, *A&AS*, 44, 109
- Hubert-Delplace, A.-M., Hubert, H., Chambon M. T., Jaschek, M. 1982 in *IAU Symp. 98 Be Stars*, Ed M. Jaschek, H.-G. Groth (Dordrecht, Reidel) p 125.
- Ignace, R., Cassinelli, J. P., & Bjorkman, J. E. 1998, *ApJ*, 505, 910
- Ignace, R., Cassinelli, J. P., & Bjorkman, J. E. 1996, *ApJ*, 459, 671
- Jaschek, C. & Jaschek, M. 1983, *A&A*, 117, 357
- Lamers, H. J. G. L. M., & Cassinelli, J. P. 1999, *Introduction to Stellar Winds*, (New York: Cambridge Univ. Press) (L & C)
- Lee, U., Saio, H., and Osaki, Y. 1991, *MNRAS*, 250, 432
- Maheswaran, M., & Cassinelli, J. P. 1988, *ApJ*, 335, 931
- Maheswaran, M., & Cassinelli, J. P. 1992, *ApJ*, 386, 695
- Marlborough, M., & Peters, G. 1986, *ApJS*, 62, 875
- McLean, I. S., & Brown, J. C. 1978, *A&A*, 69, 291
- Mestel, L. 1990, in *IAU Symp 142, Basic Plasma Processes on the Sun* (Dordrecht: Kluwer Acad. Publ.), 67
- Okazaki, A. T. 1991, *PASJ*, 43, 75

- Okazaki, A. T. 1996, PASJ, 48, 305
- Okazaki, A. T. 1997, A&A, 318, 548
- Owocki, S. P., & Cranmer, S. R. 2001, in ASP Conf. Series, Radial and Non-Radial Pulsations as Probes of Stellar Physics ed. C. Aerts et al., in press
- Owocki, S. P., Cranmer, S., & Gayley, K. G., 1996, ApJ, 472, L115
- Osterbrock, D. E. 1989, *Astrophysics of Gaseous Nebulae and Active Galactic Nuclei* (Mill Valley, CA: Univ. Sci. Books)
- Papaloizou, J. C., Savonije, G. J., Henrichs, H. F. 1992, A&A, 265, L45
- Poe, C. H., & Friend, D. B. 1986, ApJ, 311, 317
- Poe, C. H., Friend, D. B., & Cassinelli, J. P. 1989, ApJ, 337, 888
- Prinja, R. K. 1989, MNRAS, 241, 721
- Smith, M. A., Henrichs, H. F., & Fabregat, J. 2000, in IAU Coll. 175, ASP Conf Ser. 214, The Be Phenomenon in Early Type Stars, ed. M. A. Smith, H. F. Henrichs, & Fabregat, J. (ASP)
- Taylor, A. R., Waters, L. B. F. M., Bjorkman, K. S., & Dougherty, S. M. 1990, A&A, 231, 453.
- Telting, J. H. 2000, in IAU Coll. 175, ASP Conf Ser. 214, The Be Phenomenon in Early Type Stars, ed. M. A. Smith & H. F. Henrichs (ASP) 422
- Telting, J. H., Heemskerk, M. H. M., Henrichs, H. F. Savonije, G. J. 1994, A&A, 288, 558
- Waters, L. B. F. M. 1986, A&A, 162, 121
- Waters, L. B. F. M., Marlborough, J. M. 1992 A&A, 256, 195
- Wood, K., Bjorkman, K. S., & Bjorkman, J. E. 1997 ApJ, 477, 926
- Yudin, R. V. 2001, A&A, 368, 912



Table 1: Minimum fields for torqued disks around stars along the main sequence

Spectral Type	$T_{\text{eff}}$ ( $10^4$ K)	$R$ ( $10^{12}$ cm)	$M$ ( $10 M_{\odot}$ )	$\dot{M}$ ( $10^{-9} M_{\odot} \text{ yr}^{-1}$ )	$v_{\infty}$ ( $\text{km s}^{-1}$ )	$Y_*$ (G)	$B_{\odot, \text{Tth}}$		
							$\mathcal{S}_{\odot}=0.5$	$\mathcal{S}_{\odot}=0.7$	$\mathcal{S}_{\odot}=0.9$
O3	5.0	.98	5.5	9100	3100	12700	30900	22400	17900
O6.5	4.0	.70	2.9	310	2500	2830	6890	5000	4000
B0	3.2	.46	1.5	27	1300	904	2200	1600	1280
B2	2.3	.31	.83	.4	840	138	335	243	195
B5	1.5	.23	.45	.01	580	26	64	46	37
B9	1.0	.18	.26	.0013	460	11	27	20	16

Table 2: Equivalent widths of  $H_\alpha$  from torqued disks in stars along the main sequence

Spectral Type	$T_{\text{eff}}$ ( $10^4$ K)	$L(\text{H}\alpha)$ (ergs s $^{-1}$ )	$W_\lambda$ ( $\text{\AA}$ )	$\tau$	$W_\lambda e^{-\tau}$ ( $\text{\AA}$ )
O3	5.0	$3 \times 10^{40}$	$2.0 \times 10^6$	580	0.0
O6.5	4.0	$1 \times 10^{39}$	$8.2 \times 10^3$	27	$7.8 \times 10^{-9}$
B0	3.2	$9 \times 10^{37}$	114	2.4	10.65
B2	2.3	$1 \times 10^{36}$	0.089	.046	0.085
B5	1.5	$4 \times 10^{34}$	$2.4 \times 10^{-4}$	$2 \times 10^{-3}$	$2.4 \times 10^{-4}$
B9	1.0	$8 \times 10^{33}$	$1.8 \times 10^{-5}$	$3 \times 10^{-4}$	$1.8 \times 10^{-5}$

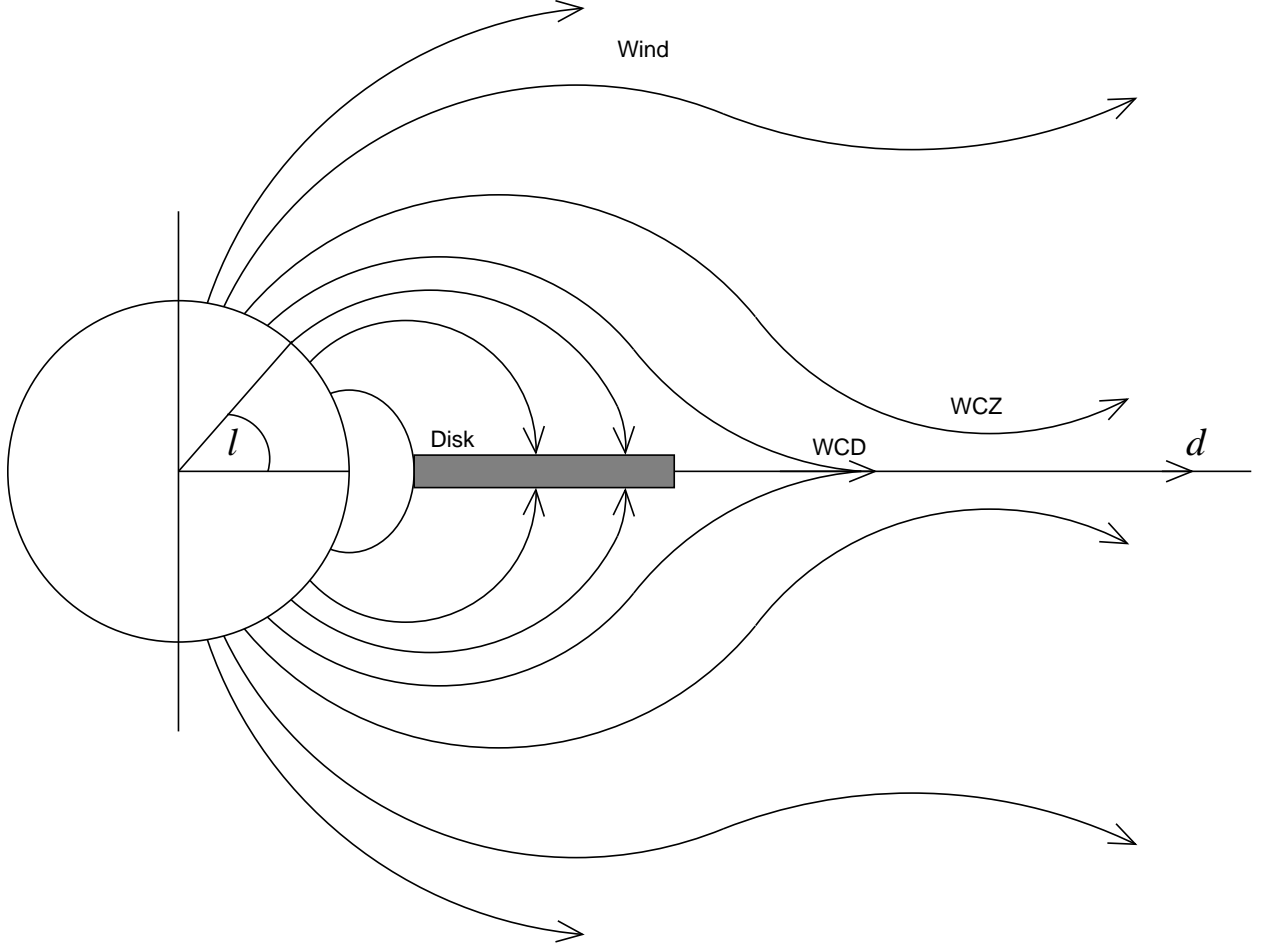


Fig. 1.— Illustrates the overall structure assumed in our Magnetically Torqued Disk model. The star has a dipole-like inner field with axis aligned with the rotation axis of the star. Material leaving the star at latitude  $l$  is channeled by the field to the equatorial disk at  $r = d(l)$ . The rotation causes the channeling process to transfer angular momentum from the star to the disk. This will lead to a distribution of angular speed  $v_\phi$  versus the equatorial distance  $d$  from the star. Note that in the outer regions the field lines are stretched and drawn out by the flow from the star.

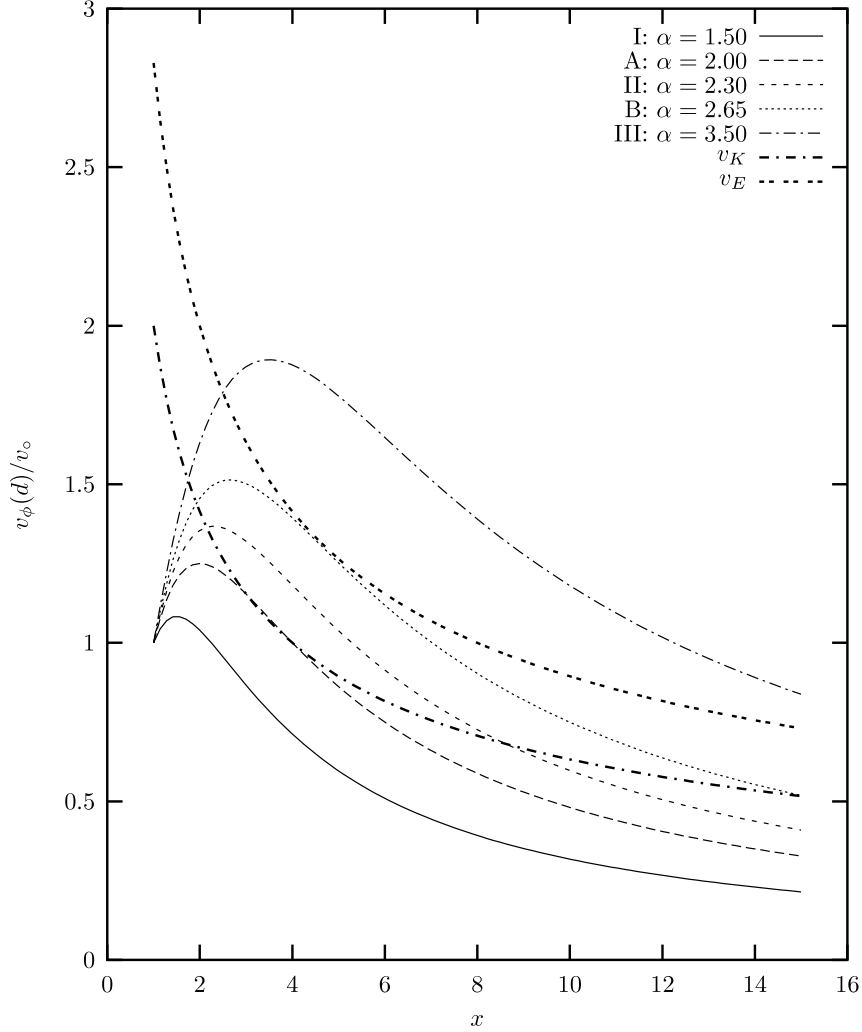


Fig. 2.— The assumed parametric distribution of  $v_\phi(d)$  versus equatorial distance. These are not flow lines but rather give the azimuthal velocity  $v_\phi(d)$  of material as it reaches the equatorial plane having started at latitude sector  $l$ . A spin rate of  $\mathcal{S}_\circ = 0.5$ , is used for this figure. In the near solid body region near the star the  $v_\phi$  for increasing  $l$  increases with distance,  $d(l)$  from the star. Note that  $\alpha$  depends on the magnetic field, the spin  $\mathcal{S}_\circ$  and outflow density in the wind. Curves for five stars of different  $\alpha$  values are shown (from Equation 7). Also shown are the Keplerian  $v_K(d)$  distribution and the parallel but larger escape speed distribution  $v_E(d)$ .

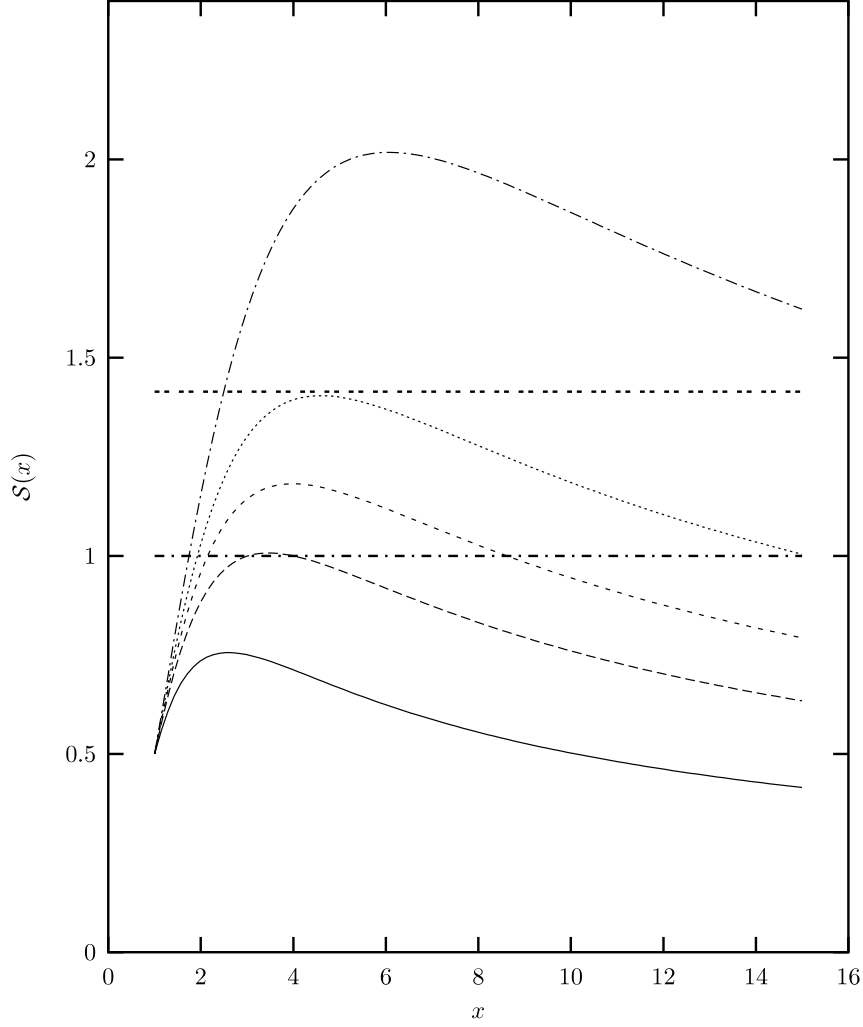


Fig. 3.— The curves of  $\mathcal{S}(x) = v_\phi(x)/v_K(x)$  for a range of  $\alpha$  and for  $\mathcal{S}_0 = 0.5$ . To contribute to a quasi-Keplerian disk the  $\mathcal{S}$  distribution must reach values of unity and above. There is a minimal value of  $\alpha$  for this to occur. For higher values of  $\alpha$ ,  $\mathcal{S}$  reaches a maximum farther out and that maximal point is taken to be the outer boundary of the magnetically dominated disk. The line types are identified in Figure 2.

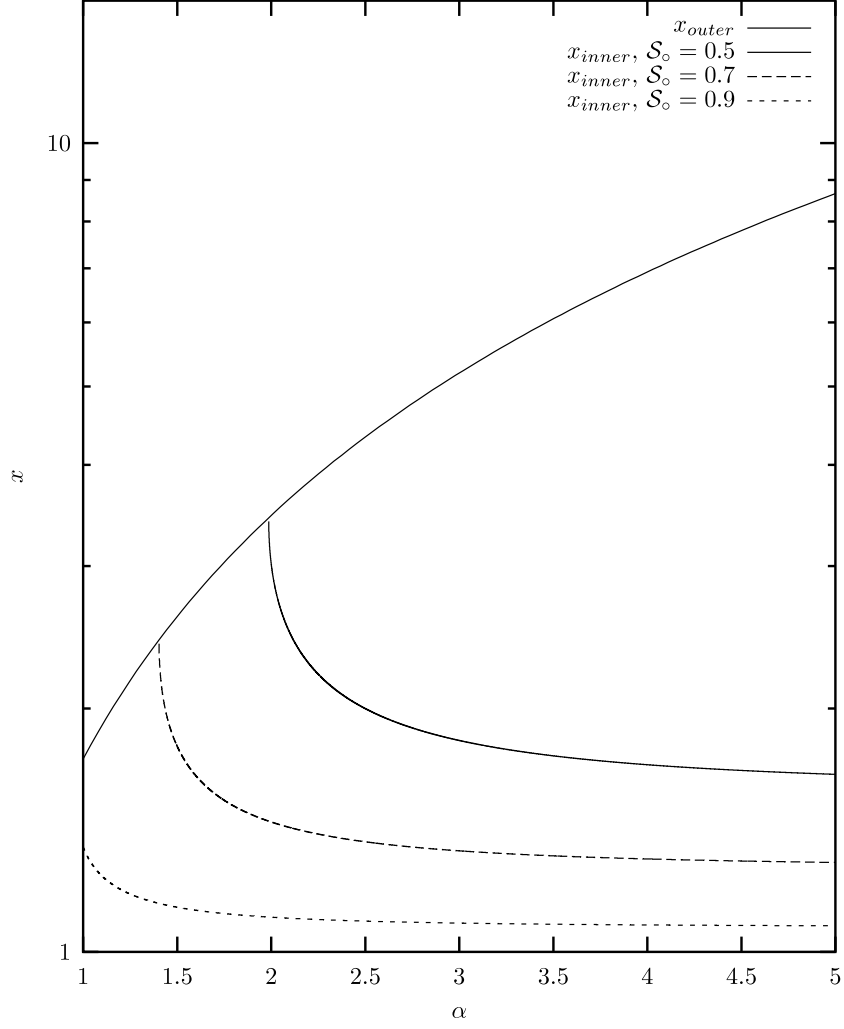


Fig. 4.— The minimal and maximal radii  $x_{inner}$  and  $x_{outer}$  as functions of  $\alpha$ . Equation 10 is used to calculate  $x_{inner}$  with the indicated values of  $\mathcal{S}_o$ , while  $x_{outer} = \sqrt{3}\alpha$ .

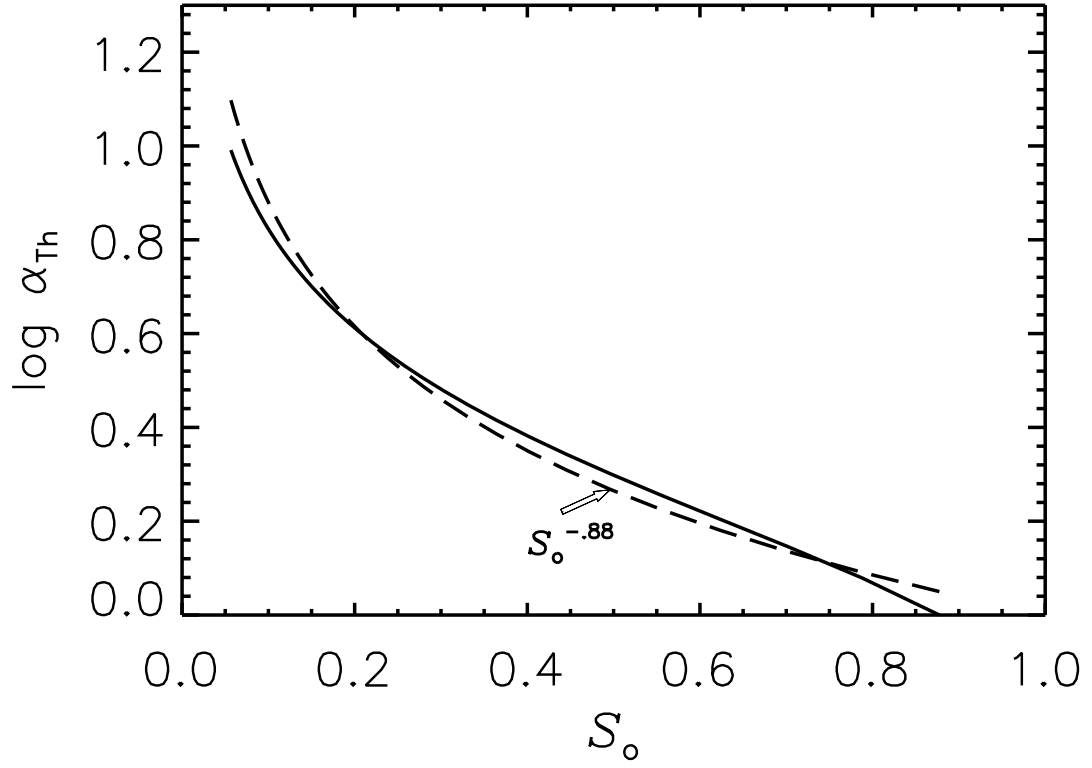


Fig. 5.— The solid line shows the dependence on the spin parameter  $S_o$  of the minimal value of  $\alpha$  ( $= \alpha_{Th}$ ) required for disk formation, as given by Eq. (15). The dashed line illustrates the good fit given by the power law expression described by Eq. (16).

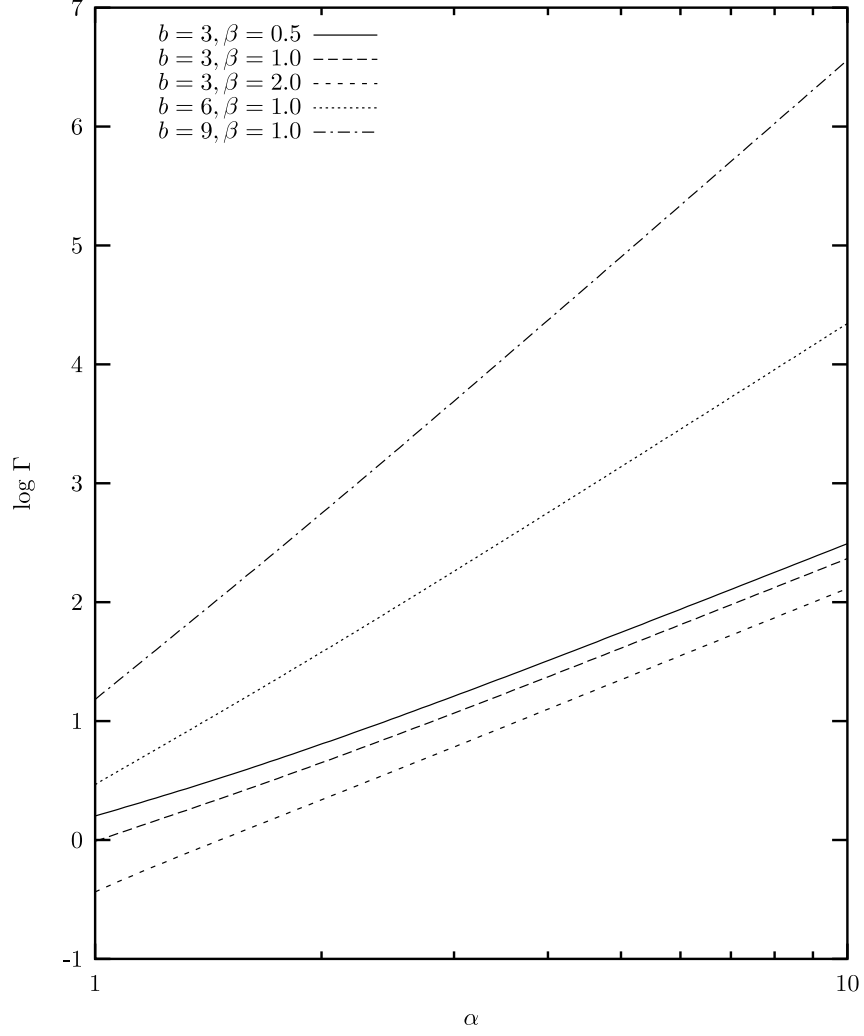


Fig. 6.— The function  $\Gamma(\alpha)$  (Eq. (36)) is shown for the values of  $b$  and  $\beta$  as described by the different line styles in the legend. The case  $b = 3$  corresponds to a dipole magnetic field.



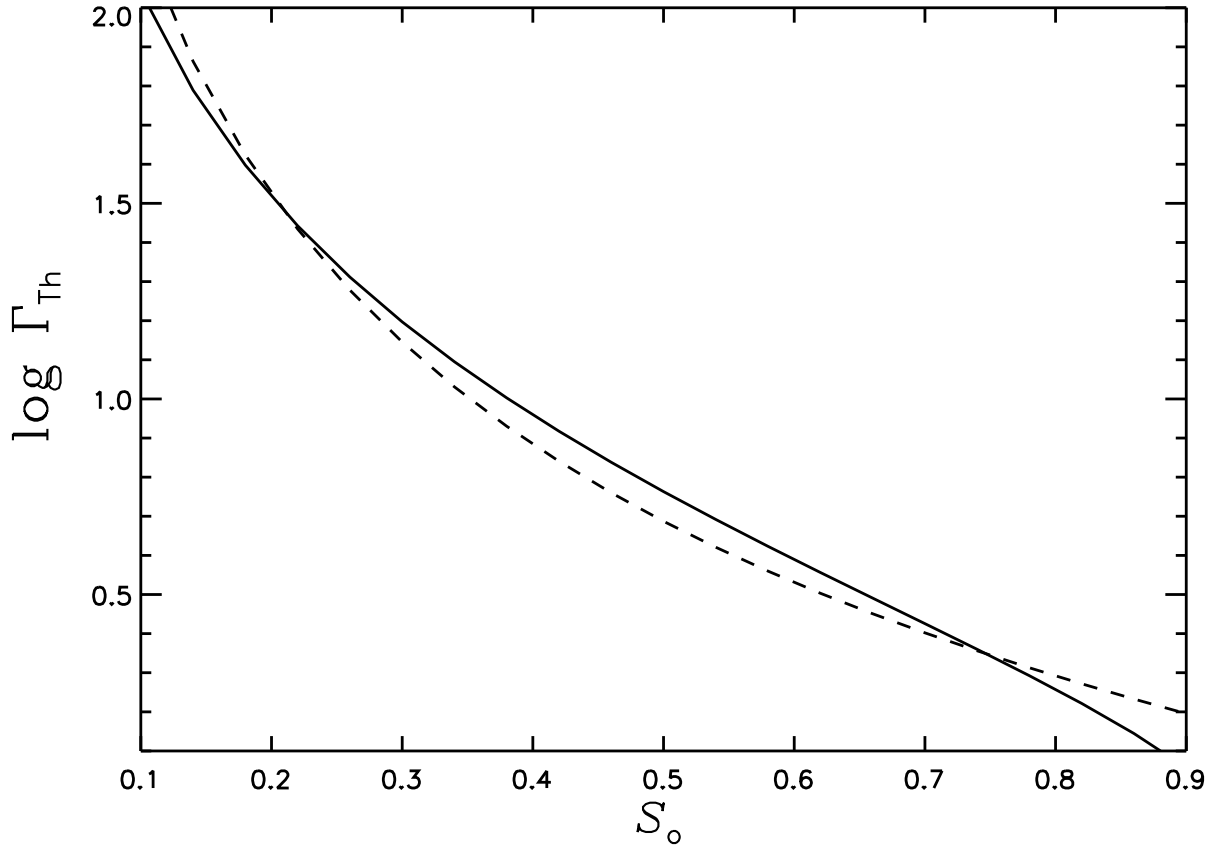


Fig. 7.— The threshold value of  $\Gamma$  versus  $\mathcal{S}_0$  for  $b = 3$  and for  $\beta = 1.0$ , from empirical Equation (42) (dashed line) and also from the exact solution of Equations (15) and (35) (solid line).

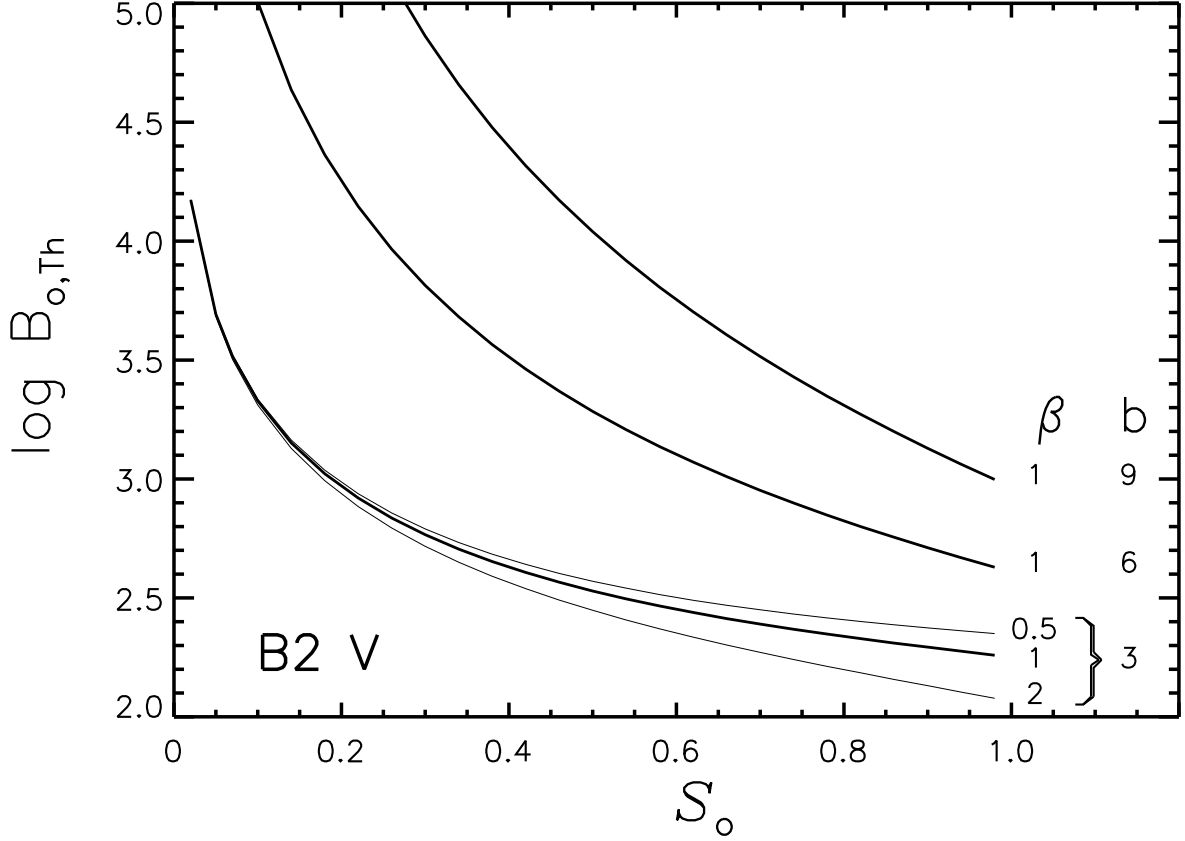


Fig. 8.— The minimal or threshold surface magnetic field for the formation of a disk versus  $S_o$  for which we have used the parameters of a B2V star from Table 1. The different curves illustrate the effects of varying the model parameters,  $b$ , which gives the radial dependence of the magnetic field, and  $\beta$ , which is the outflow velocity law parameter. For a case in which the field drops more sharply with distance from the star the required surface field needs to be larger. Three values of  $\beta$  are shown for the  $b = 3$  case. The slower the rise in velocity, (e.g.  $\beta = 2$ ) the smaller the field needed to produce the torqued disk, for a given  $S_o$ .

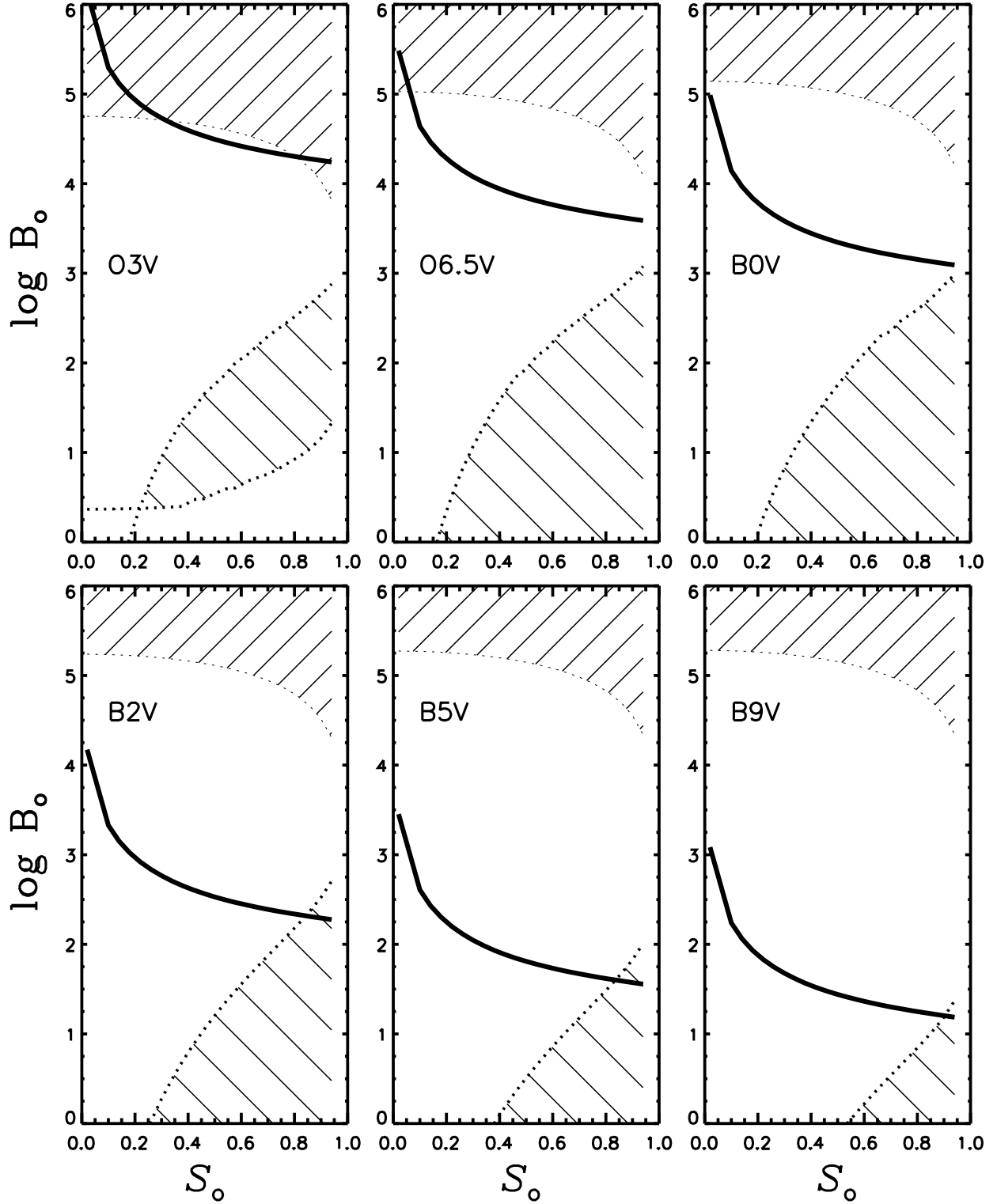


Fig. 9.— Shows the limits derived for the maximal and minimal field strengths for Be stars versus  $S_0$  derived from photospheric constraints of Maheswaran & Cassinelli (1992). The solid line shows the minimal  $B_0$  as a function of  $S_0$  such that a disk can be magnetically torqued; for these calculations we use the stellar parameters from Table 1,  $b = 3$ , and  $\beta = 1$ .

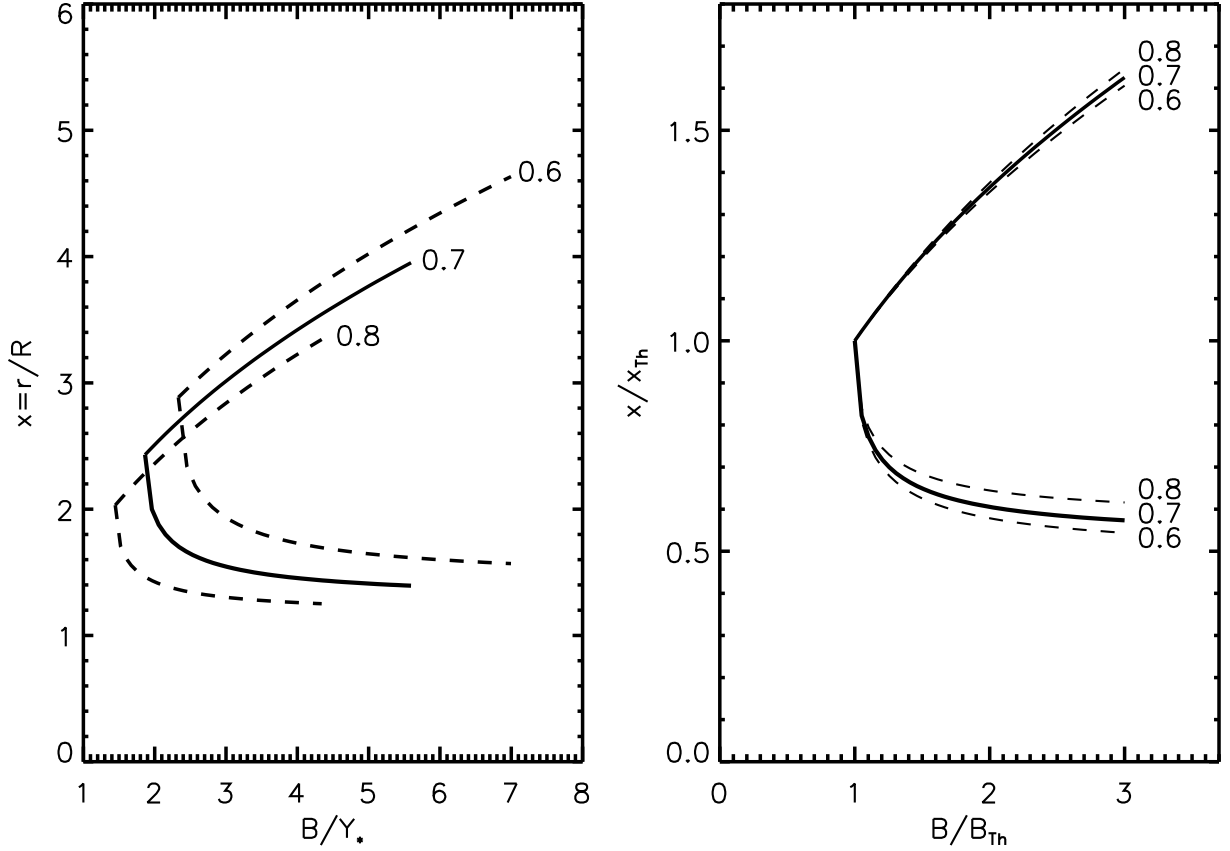


Fig. 10.— Two panels that show the radial extent ( $x_{\text{inner}}$  to  $x_{\text{outer}}$ ) of magnetically torqued disks versus the surface magnetic field,  $B_{\text{o}}$ . The  $B$  field is normalized in units of  $Y_*$ , so the plot is applicable to any star. a) In the left panel results for the boundaries are shown for three values of the spin rate parameter  $\mathcal{S}_{\text{o}}$ . The upper segments of the curves correspond to  $x_{\text{outer}}$  and note these merge with the lower segments, the  $x_{\text{inner}}$  curves, at the threshold point for each of the three models. The curves appear very similar in shape although shifted. b) To illustrate the homologous nature of the curves, in the right panel is shown the quantities on both axes in the left panel are normalized by the threshold values. Notice that the extent of the disk ( $x_{\text{outer}} - x_{\text{inner}}$ ) increases sharply for magnetic fields just above the threshold value.

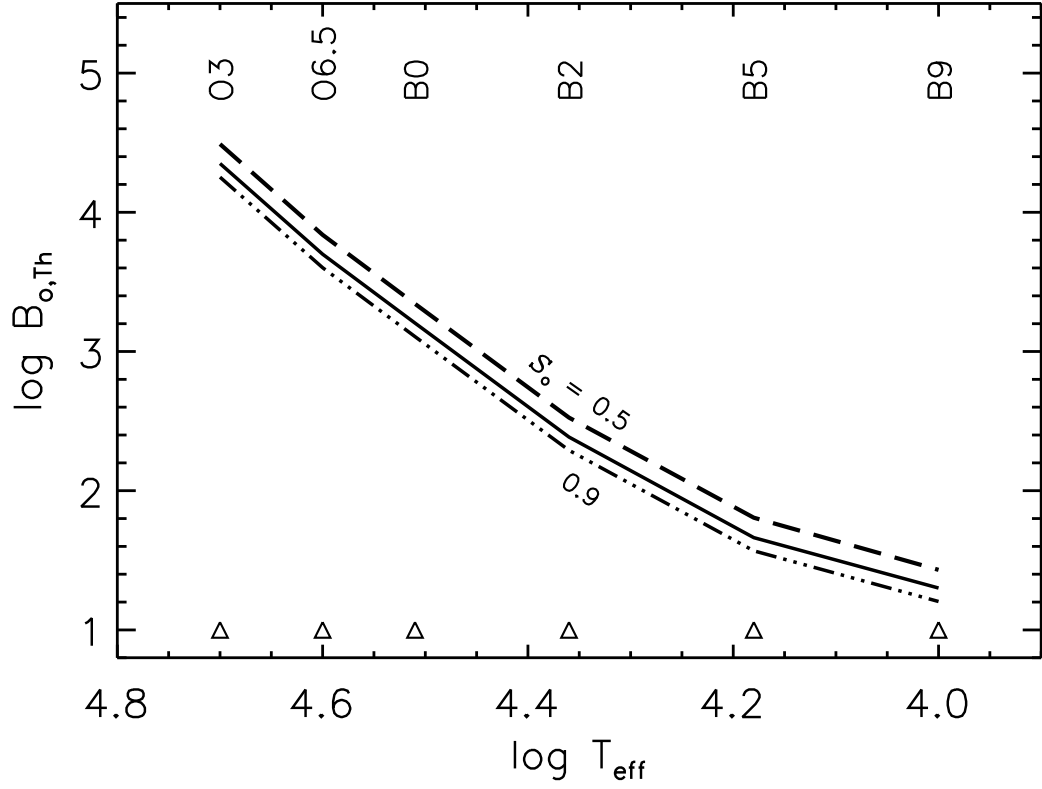


Fig. 11.— Shows the threshold field for torqued disks for stars along the main sequence. The stellar parameters are from Table 1 and  $b = 3$ ,  $\beta = 1$  are assumed. The three curves correspond to the values of the spin rate  $\mathcal{S}_o = 0.5, 0.7$  and  $0.9$ , two of which are labeled.

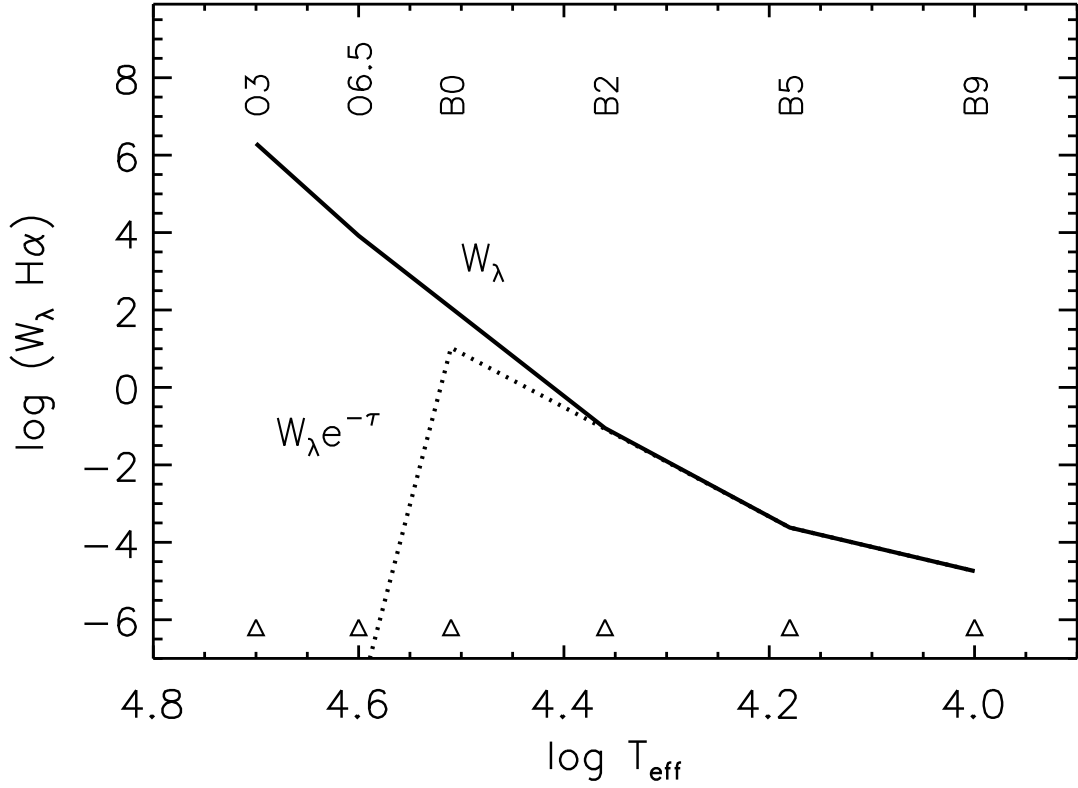


Fig. 12.— The solid line shows an estimate of the upper limit to the equivalent width of the  $H\alpha$  line in  $\text{\AA}$  versus  $T_{\text{eff}}$ , produced in a disk of infinite extent. The dotted line shows the reduced value of the equivalent width when optical depths in the disk are accounted for in an approximate way. The unmodified  $W_\lambda$  indicates unacceptably large values for the early type stars, however, for these stars the magnetic field required would also be excessively large (i.e. greater than a kilogauss).